

RESEARCH

Open Access



# Spatiotemporal characterization of aerosols and trace gases over the Yangtze River Delta region, China: impact of trans-boundary pollution and meteorology

Zeeshan Javed<sup>1†</sup>, Muhammad Bilal<sup>2†</sup>, Zhongfeng Qiu<sup>2</sup>, Guanlin Li<sup>1</sup>, Osama Sandhu<sup>3</sup>, Khalid Mehmood<sup>4</sup>, Yu Wang<sup>2</sup>, Md. Arfan Ali<sup>2</sup>, Cheng Liu<sup>5,6,7,8</sup>, Yuhang Wang<sup>9</sup>, Ruibin Xue<sup>10</sup>, Daolin Du<sup>1\*</sup> and Xiaojun Zheng<sup>1\*</sup>

## Abstract

**Background:** The spatiotemporal variation of observed trace gases ( $\text{NO}_2$ ,  $\text{SO}_2$ ,  $\text{O}_3$ ) and particulate matter ( $\text{PM}_{2.5}$ ,  $\text{PM}_{10}$ ) were investigated over cities of Yangtze River Delta (YRD) region including Nanjing, Hefei, Shanghai and Hangzhou. Furthermore, the characteristics of different pollution episodes, i.e., haze events (visibility  $< 7$  km, relative humidity  $< 80\%$ , and  $\text{PM}_{2.5} > 40 \mu\text{g}/\text{m}^3$ ) and complex pollution episodes ( $\text{PM}_{2.5} > 35 \mu\text{g}/\text{m}^3$  and  $\text{O}_3 > 160 \mu\text{g}/\text{m}^3$ ) were studied over the cities of the YRD region. The impact of China clean air action plan on concentration of aerosols and trace gases is examined. The impacts of trans-boundary pollution and different meteorological conditions were also examined.

**Results:** The highest annual mean concentrations of  $\text{PM}_{2.5}$ ,  $\text{PM}_{10}$ ,  $\text{NO}_2$  and  $\text{O}_3$  were found for 2019 over all the cities. The annual mean concentrations of  $\text{PM}_{2.5}$ ,  $\text{PM}_{10}$ , and  $\text{NO}_2$  showed continuous declines from 2019 to 2021 due to emission control measures and implementation of the Clean Air Action plan over all the cities of the YRD region. The annual mean  $\text{O}_3$  levels showed a decline in 2020 over all the cities of YRD region, which is unprecedented since the beginning of the China's National environmental monitoring program since 2013. However, a slight increase in annual  $\text{O}_3$  was observed in 2021. The highest overall means of  $\text{PM}_{2.5}$ ,  $\text{PM}_{10}$ ,  $\text{SO}_2$ , and  $\text{NO}_2$  were observed over Hefei, whereas the highest  $\text{O}_3$  levels were found in Nanjing. Despite the strict control measures,  $\text{PM}_{2.5}$  and  $\text{PM}_{10}$  concentrations exceeded the Grade-1 National Ambient Air Quality Standards (NAAQS) and WHO (World Health Organization) guidelines over all the cities of the YRD region. The number of haze days was higher in Hefei and Nanjing, whereas the complex pollution episodes or concurrent occurrence of  $\text{O}_3$  and  $\text{PM}_{2.5}$  pollution days were higher in Hangzhou and Shanghai.

The in situ data for  $\text{SO}_2$  and  $\text{NO}_2$  showed strong correlation with Tropospheric Monitoring Instrument (TROPOMI) satellite data.

**Conclusions:** Despite the observed reductions in primary pollutants concentrations, the secondary pollutants formation is still a concern for major metropolises. The increase in temperature and lower relative humidity favors the

<sup>†</sup>Zeeshan Javed and Muhammad Bilal contributed equally to this work

\*Correspondence: ddl@ujs.edu.cn; xjzheng@ujs.edu.cn

<sup>1</sup>Institute of Environment and Ecology, School of the Environment and Safety Engineering, Jiangsu University, Zhenjiang 212013, China  
Full list of author information is available at the end of the article

accumulation of  $O_3$ , while low temperature, low wind speeds and lower relative humidity favor the accumulation of primary pollutants. This study depicts different air pollution problems for different cities inside a region. Therefore, there is a dire need to continuous monitoring and analysis of air quality parameters and design city-specific policies and action plans to effectively deal with the metropolitan pollution.

**Keywords:** Yangtze River Delta region, Ozone, Particulate matter, China's clean air action plan, TROPOMI, National Ambient Air Quality Standards

## Background

Rapid urbanization and industrialization, deteriorating the air quality of most Chinese cities have resulted in adverse impacts on public health [1–3]. According to the World Health Organization [WHO] standards, only 1% of Chinese megacities meet the safe city criteria in terms of air quality [4]. Atmospheric aerosols unswervingly impact the earth's radiation budget, ecological environment, human health, and climate [5]. Atmospheric pollution is caused by higher concentrations of various trace gas species including the oxides of nitrogen ( $NO_x$ ) and sulfur ( $SO_x$ ), tropospheric ozone ( $O_3$ ), volatile organic compounds (VOCs), and airborne particulate matter [PM], which pose serious threats to human health [6–8]. The primary emissions from anthropogenic sources are the trace gases such as  $NO_2$ ,  $SO_2$ , and carbon monoxide (CO) [9]. Industrial emissions, fossil fuel combustion, and biofuels act as the major sources of  $SO_2$  and CO [10]. Both CO and  $NO_x$  act as the main precursors of  $O_3$ , whereas  $NO_x$  and  $SO_2$  are significant towards the production of secondary inorganic aerosols [11]. The pollution sources have a significant impact on aerosol properties and are driven by atmospheric oxidation capacity, the intensity of emissions, and meteorological conditions. The role of meteorological parameters on different pollution episodes have been documented in previously reported studies [11]. Despite ample research on the effects of meteorological parameters on atmospheric pollution, significant variation in the intensity and extent of these impacts exists for different seasons and across different regions.

China has established more than 1500 stations for air quality monitoring since 2013, with a prime focus on monitoring different trace gases and particulate matter, i.e.,  $PM_{2.5}$ ,  $PM_{10}$ ,  $NO_2$ ,  $SO_2$ ,  $O_3$ , and CO [10–13]. The measurements taken at these monitoring stations have been used to analyze the characteristics of different air pollution episodes in various regions of China including the Yangtze River Delta (YRD) region [10–12, 14].

The YRD region is located adjacent to the North China Plain (NCP) and experiences complicated environmental pollution issues originating from dust plumes, biomass burning, photochemical reactions,

and coal combustion [15]. The occurrence of severe haze episodes in the YRD region is one of these environmental pollution issues [16–18]. Haze is a condition that obstructs visual range and is defined as the weather phenomenon that leads to a reduction in atmospheric visibility caused by the accumulation of suspended solid or liquid fine particles [19–21]. The other major pollution issue in the YRD region is a phenomenon in which high  $O_3$  and high  $PM_{2.5}$  coincided beyond the National Ambient Air Quality Standards (NAAQS) [14, 22, 23]. This condition is termed as a complex pollution in this study hereafter, where the daily averaged  $PM_{2.5}$  concentration exceeds  $35 \mu\text{g}/\text{m}^3$ , and the daily averaged  $O_3$  concentration exceeds  $160 \mu\text{g}/\text{m}^3$  on the same day.

The effects of cross-boundary air pollution and climatic factors on air quality are reported in different cities of the YRD region [24–27]. Though these investigations were either limited to specific particulate matter, trace gases, time intervals, or certain regions of YRD, the variation among various cities of YRD and their influential factors are not still clear. Thus, it is imperative to study the recent spatiotemporal distribution and characteristics of the criteria pollutants at different geographical locations within YRD. This is the first comprehensive study analyzing different air pollution episodes across YRD regions using recent datasets from National environmental monitoring centers. The study broadly characterizes the current air quality status, over the four most polluted and populous cities of YRD during 2018–2021. This research (a) examines the recent long-term temporal variation of trace gases and particulate matter (b) impact of different meteorological parameters on pollutants (c) identifies different pollutant sources using PSCF (Potential Source Contribution Function) with HYSPLIT (Hybrid Single-Particle Lagrangian Integrated Trajectory) back trajectory analysis (d) in situ measurements of  $SO_2$  and  $NO_2$  are compared with TROPOMI satellite data. Further, haze and complex pollution episodes over the study region were also analyzed. The outcomes of this up-to-date study could provide a wide-ranging logical and scientific basis for decision-making while designing effective air pollution control policies for metropolises.

## Methods

### Description of the study area

Anhui, Jiangsu, Shanghai, and Zhejiang are the major provinces that mainly cover the eastern side of the Yangtze plain. Fertile plains make this area characteristically unique and deem it suitable for a variety of food as well as cash crops. According to statistics, the gross domestic product (GDP) exceeded over USD 2.2 trillion for the YRD region as of 2018 (China Statistics: <http://data.stats.gov.cn/english>, accessed on 26 December 2021). The total area covered by the YRD region sums up to be 210,700 km<sup>2</sup> and supports a huge population numbered about 0.23 billion in 2018 [28]. The vulnerability of the region to excessive atmospheric pollution comes from the high industrial growth, economic activity, and ever-increasing population which enhances the anthropogenic footprint on the environment. The four most important cities of the YRD region have been observed in this study, including Hangzhou, Hefei, Nanjing, and Shanghai. All of these have a very high population density and are the hubs for industrial and economic activities which make them prone to extreme pollution episodes. Figure 1 shows the location of these above-mentioned megacities in the YRD region.

### Data sets

#### *In situ measurements and meteorological parameters*

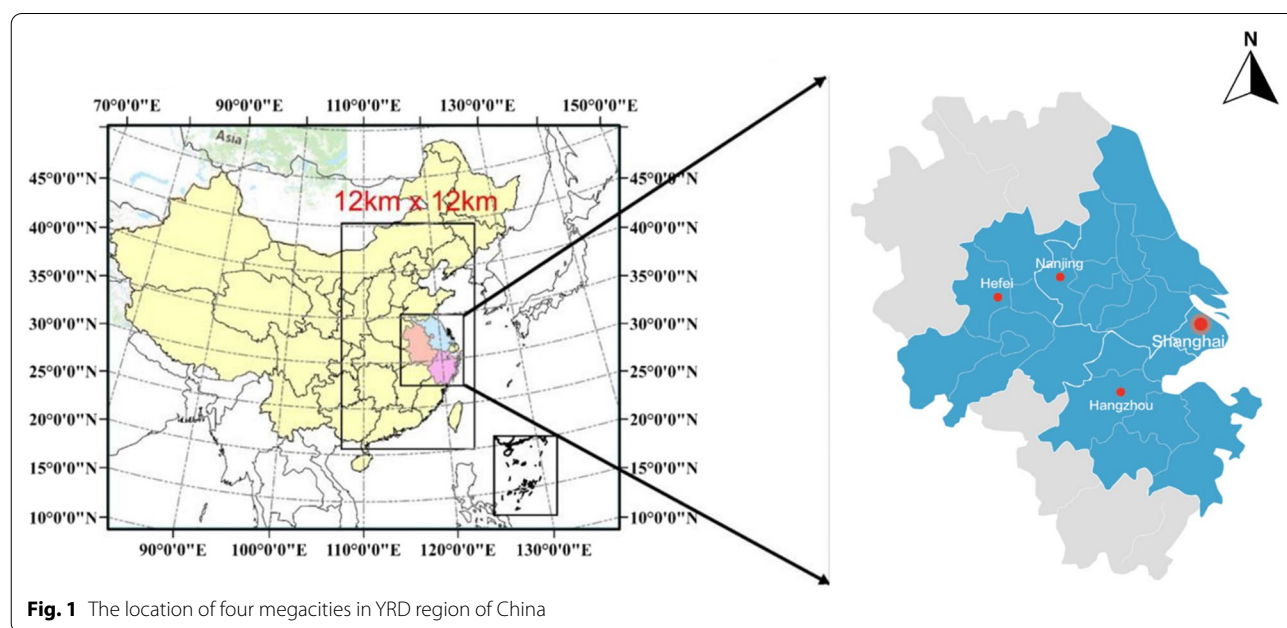
In situ measurements were attained via a National online database for air quality analysis and monitoring platform for NO<sub>2</sub>, PM<sub>2.5</sub>, PM<sub>10</sub>, SO<sub>2</sub>, and MDA8 O<sub>3</sub> (Maximum Daily 8-hour Average Ozone). The data are available

online and the monitoring stations are managed by China National Environmental Monitoring Center. The instruments deployed at these monitoring centers accord to the China Environmental Protection Standard HJ 664-2013. National ambient air quality standards (GB 3095e2012; China) were used to check the validity of the data, as reported in the previous study [12]. The hourly mean data of 10 different monitoring stations over each city (Additional file 1: Table S1) were used from 2018 to 2021. The city-wide day-to-day mean level of pollutants was estimated by taking an average of all the monitoring stations over a particular city as reported in previous studies [29]. The quality control approaches were applied to filter the problematic data as described in previous studies [30].

Meteorological parameters including temperature, visibility, relative humidity and wind speed were taken into account for the aforementioned time frame. Automatic weather stations installed at respective airports of each city were used to obtain meteorological data.

#### *TROPOMI*

TROPOMI level-2 NO<sub>2</sub> and SO<sub>2</sub> product published by Royal Netherlands Meteorological Institute (KNMI) has been used for the current study. Differential optical absorption spectroscopy (DOAS) algorithm is used to retrieve tropospheric VCDs following three major steps: 1) retrieval of slant column densities (SCDs), 2) differentiating stratospheric SCDs from tropospheric SCDs, and 3) converting SCDs to VCDs using air mass factor (AMF). Owing to the error linked to the calculation of



AMF, an obvious underestimation of TROPOMI tropospheric NO<sub>2</sub> and SO<sub>2</sub> has been reported in recent studies, especially in polluted regions. In order to ensure reliability, the data with quality flag exceeding 0.75 were used for this study.

## Methodology

### Categorization of different pollution episodes

**Haze pollution** To investigate the impact of haze days on PM<sub>2.5</sub>, PM<sub>10</sub>, NO<sub>2</sub>, SO<sub>2</sub>, and O<sub>3</sub> over the study region, the study period has been divided into the haze and non-haze days. Haze days were defined with visibility < 7.5 km, RH < 80%, and PM<sub>2.5</sub> > 40 µg/m<sup>3</sup>, while non-haze days were defined with visibility > 7.5 km, RH < 80%, and PM<sub>2.5</sub> < 40 µg/m<sup>3</sup> non-haze. A similar categorization of Haze and non-haze days is reported in different studies [19, 20, 31]. The aforementioned categorization for haze and non-haze days has been used for the current study over main cities of the YRD region including Hangzhou, Hefei, Nanjing, and Shanghai.

**Complex pollution** The complex pollution days refer to the pollution conditions where the daily averaged PM<sub>2.5</sub> concentration exceeds 35 µg/m<sup>3</sup>, and the daily averaged O<sub>3</sub> concentration exceeds 160 µg/m<sup>3</sup> on the same day. This categorization is used in this study over cities of the YRD region including Hangzhou, Hefei, Nanjing, and Shanghai.

### Principal component analysis

Possible pollutant sources can be explored by employing principal component analysis (PCA) along with the study of the correlations among the pollutant concentrations. PCA was employed using SPSS v17.0 for five air pollutants with daily mean data points for each variable. The numbers of principal components (PCs) are determined by the variability in the data and frequency of inspected elements. PCA exploits the factor loading of each variable, which is why it was used with Varimax rotation [32] as reported in the earlier study [33].

### Potential source contribution function

The origin of air masses was determined by performing backward trajectory analysis by employing the Hybrid Single-Particle Lagrangian Integrated Trajectory (HYSPLIT) model established by National Oceanic and Atmospheric Administration (NOAA) [34]. A comprehensive understanding of the transport of air masses, their dispersion, and chemical conversion is offered by this model [35] which also highlights the probable causes of aerosol pollutants that impact the air quality. The integration of HYSPLIT backward trajectory with PSCF analysis and daily SO<sub>2</sub>, NO<sub>2</sub>, O<sub>3</sub>, PM<sub>2.5</sub>, and PM<sub>10</sub>

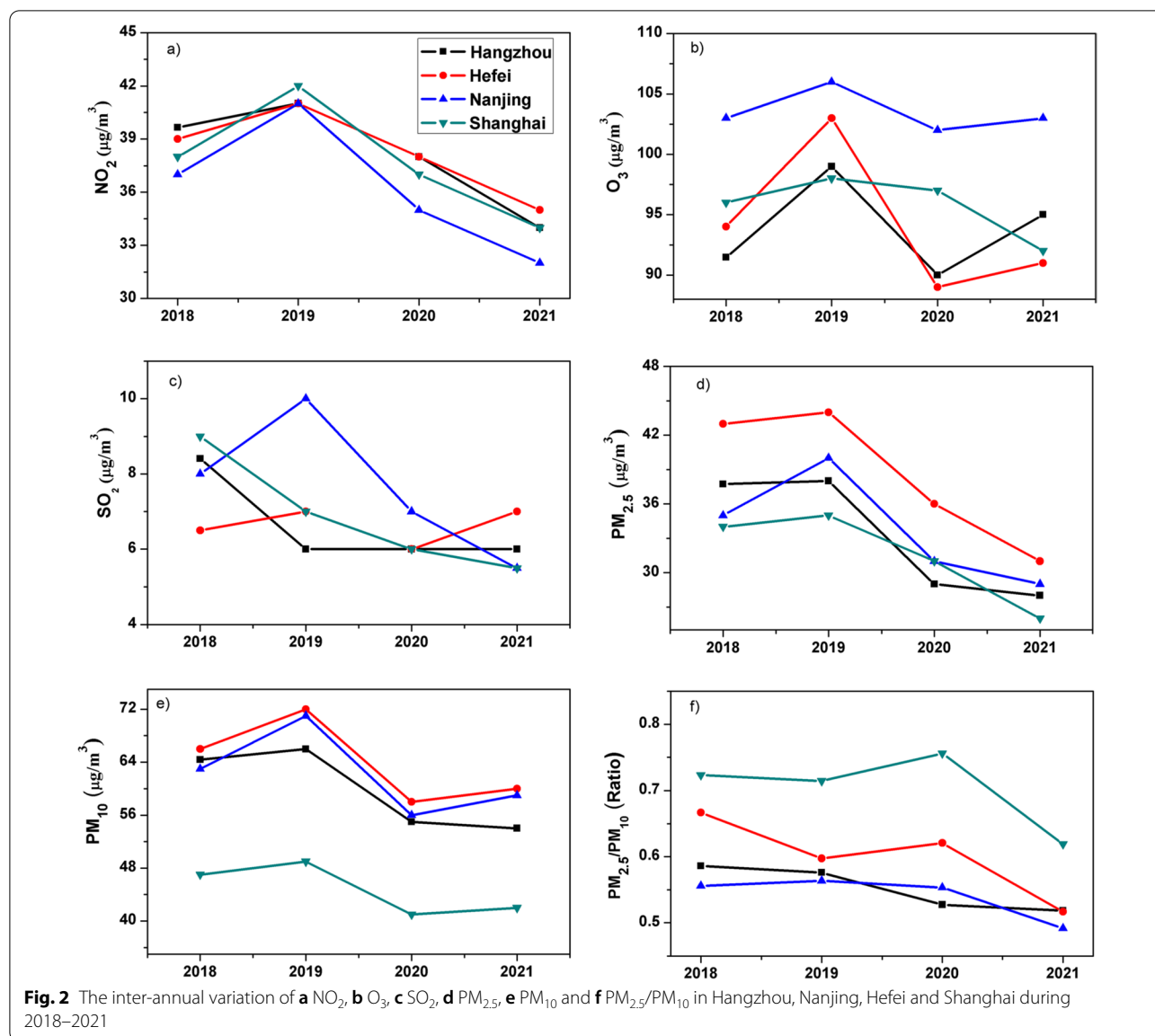
measurements over a grid of 0.5°×0.5 degrees was carried out to find the source strength of different geographical locations. The trajectory was calculated (72 h for every 6 h) at a height of 500 m above the ground level (AGL) employing meteorological data from the GDAS (Global Data Assimilation System) on 1° × 1° spatial resolution (accessed from: <ftp://arlftp.arlhq.noaa.gov/pub/archives/gdas1>) for each season from January 2018 to December 2021. Weighting functions were performed to lessen the uncertainty of PSCF and denoted as WPSCF [36, 37].

## Results and discussion

### Temporal variation

The time-series for yearly mean and inter-annual temporal trends of NO<sub>2</sub>, MDA8 O<sub>3</sub>, SO<sub>2</sub>, PM<sub>2.5</sub>, PM<sub>10</sub>, and PM<sub>2.5</sub>/PM<sub>10</sub> from 2018–2021 are shown in Fig. 2. The basic statistics (annual mean, maxima, minima, standard deviation, and median) of the daily mean (2018–2021) NO<sub>2</sub>, MDA8 O<sub>3</sub>, SO<sub>2</sub>, PM<sub>2.5</sub>, and PM<sub>10</sub> are shown in Additional file 1: Tables S2–S5 for Hefei, Nanjing, Shanghai, and Hangzhou. The main sources for NO<sub>2</sub> production are generally vehicular emissions, biomass burning, fossil fuel combustion, and industrial emissions [36, 38]. The highest annual mean NO<sub>2</sub> concentration (42 µg/m<sup>3</sup>) over Shanghai was observed in 2019, whereas 19% decline was observed from 2019 to 2021. Similar temporal variations were observed over other cities, i.e., the highest annual mean NO<sub>2</sub> concentration was observed in 2019 and decreased by 17%, 21%, and 14% over Hangzhou, Nanjing, and Hefei, respectively, from 2019 to 2021. Only in 2019, the mean NO<sub>2</sub> concentrations exceed the National Ambient Air Quality Standards (NAAQS < 40 µg/m<sup>3</sup>) and World Health organization Standards (WHO < 40 µg/m<sup>3</sup>) over all the cities. However, for the rest of the years, all the cities meet the NAAQS and WHO air quality standards for NO<sub>2</sub>. The decreasing trend in NO<sub>2</sub> can be accredited to the efficacy of emission control measures and implementation of the Clean Air Action plan of China. The regulation of NO<sub>x</sub> emissions from power plants played an important role in the reduction of NO<sub>2</sub> [39]. Overall, these results show that Hefei (38.4 µg/m<sup>3</sup>) is the most polluted city of the YRD region compared to the other cities, however, all the cities meet the NAAQS and WHO air quality standards based on annual mean NO<sub>2</sub> concentrations from 2018 to 2021.

SO<sub>2</sub> is mainly produced from fossil fuel burning for domestic heating, power plants emissions, oil refineries, and metal smelters [40]. Across the four cities, the highest annual mean SO<sub>2</sub> concentration (10 µg/m<sup>3</sup>) was observed in Nanjing during 2019. The annual mean concentration of SO<sub>2</sub> in Nanjing decreased by 45% from 2019 to 2021. The temporal variation of SO<sub>2</sub> over different cities of the YRD region showed contrasting results. The



maxima for Hangzhou and Shanghai (8.5 and 9 μg/m<sup>3</sup>) were observed in 2018, whereas the decline was 28% and 38%, respectively, from 2018 to 2021. The annual mean SO<sub>2</sub> concentration from 2018 to 2021 in Hefei on a whole ranged from 6 to 7 (μg/m<sup>3</sup>). The highest value 7 μg/m<sup>3</sup> was observed in both 2018 and 2021. The SO<sub>2</sub> concentration in all the cities was below the NAAQS (20 μg/m<sup>3</sup>) and WHO (20 μg/m<sup>3</sup>) guidelines. Additional file 1: Table S6 shows the China NAAQS and WHO guidelines for different trace gases and particulate matter. Previous studies also reported a decline in mean SO<sub>2</sub> concentration over different regions of China [12]. Concerning, the most polluted city during 2018–2021 in terms of SO<sub>2</sub> pollution was Nanjing with an overall mean concentration

of 7.6 μg/m<sup>3</sup>. The reduction in SO<sub>2</sub> levels over the YRD region can be linked to the strong and effective measures taken to reduce the SO<sub>2</sub> level. The previous study reported a decrease in industrial SO<sub>2</sub> emissions following the widespread installation of fuel gas desulfurization (FGD) devices in China [41].

Temporal variations of PM<sub>2.5</sub> concentrations show a similar pattern as NO<sub>2</sub>, i.e., the highest and lowest annual mean concentrations in 2019 and 2021, respectively. The annual mean PM<sub>2.5</sub> concentration decreased from 2019 to 2021 by 29%, 27%, 26%, and 25% over Hefei, Nanjing, Hangzhou, and Shanghai, respectively. The lowest mean yearly concentration of PM<sub>2.5</sub> (26 μg/m<sup>3</sup>) was observed in Shanghai. The PM<sub>2.5</sub> concentration was substantially

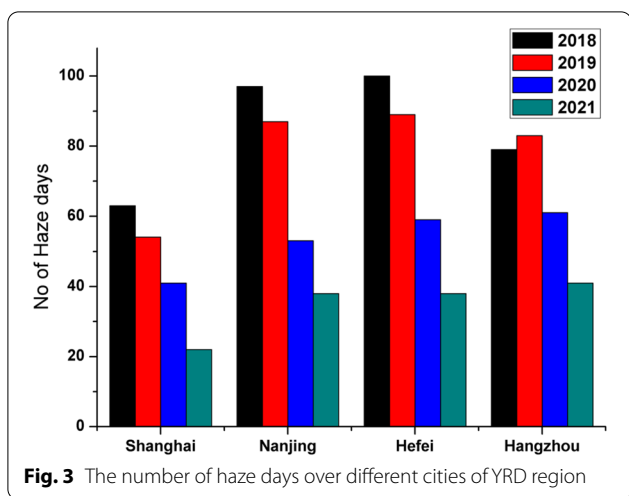


**Fig. 3** The number of haze days over different cities of YRD region

reduced over all the YRD cities. Similar findings were reported in earlier studies [22, 42]. The air pollution prevention and control action plan launched by the Chinese government in 2013 has helped in significant PM<sub>2.5</sub> emission abatements. However, the yearly mean concentration of PM<sub>2.5</sub> still exceeds the Grade 1 annual NAAQS (15 µg/m<sup>3</sup>) and WHO (15 µg/m<sup>3</sup>) air quality guidelines over all the cities.

The yearly mean PM<sub>10</sub> concentration for all the cities varies abruptly, i.e., PM<sub>10</sub> concentration increased in 2019 compared to 2018, decreased in 2020, and then again increased in 2021. However, the lowest annual mean PM<sub>10</sub> was noted in 2020. The highest annual mean PM<sub>10</sub> (72 µg/m<sup>3</sup>) was observed in 2019 over Hefei compared to the other cities. The annual mean PM<sub>10</sub> levels were beyond the grade 1 NAAQS (40 µg/m<sup>3</sup>) and WHO (15 µg/m<sup>3</sup>) guidelines over all the cities of YRD. This indicates that all the cities are facing severe air pollution problems in terms of PM<sub>2.5</sub> and PM<sub>10</sub>.

The highest annual mean concentration of MDA8 O<sub>3</sub> (106 µg/m<sup>3</sup>) was observed in 2019 over Nanjing. There has been an unprecedented reduction in average O<sub>3</sub> concentrations during 2020 over all the cities of YRD, while the previously reported studies depicted a continuous increase of approximately 5% in annual mean concentration from 2013 to 2019 over different parts of China [22, 43]. However, a recent study also reported an exceptional reduction of approximately 6% in summer time MDA8 O<sub>3</sub> during 2020 compared to 2019 over different Chinese cities [44]. This unprecedented decline in MDA8 O<sub>3</sub> during 2020 can be linked to the fact that a recent study reported a shift in ozone sensitivity from the VOC (volatile organic compounds) limited regime to the transitional regime over eastern China [45] indicating that concurrent control of both NO<sub>x</sub> and VOCs would benefit

**Table 1** Comparison of criteria pollutants during haze and non-haze days (2018–2021) over the YRD region cities

Cities	Pollutant		Percent change [H-N]/N*100
	Haze days[H]	Non-haze days[N]	
	<b>Mean PM<sub>2.5</sub> concentrations [µg/m<sup>3</sup>]</b>		
	Haze days[H]	Non-haze days[N]	[H-N]/N*100
Shanghai	77	28	175%
Nanjing	60	27	122%
Hefei	45	26	73%
Hangzhou	48	28	72%
	<b>Mean SO<sub>2</sub> concentrations [µg/m<sup>3</sup>]</b>		
Shanghai	10	07	42%
Nanjing	9.7	8.5	15%
Hefei	7	6.25	12%
Hangzhou	7.77	6.75	15%
	<b>Mean NO<sub>2</sub> concentrations [µg/m<sup>3</sup>]</b>		
Shanghai	56	35	60%
Nanjing	48	33.5	45%
Hefei	45	35	28%
Hangzhou	47	32	46%
	<b>Mean PM<sub>10</sub> concentrations [µg/m<sup>3</sup>]</b>		
Nanjing	95	60	58%
Hefei	75	57	31%
Hangzhou	80	52.5	53%
	<b>Mean O<sub>3</sub> concentrations [µg/m<sup>3</sup>]</b>		
Shanghai	94	103	− 9%
Nanjing	93	123	− 32%
Hefei	90	113	− 25%
Hangzhou	85	111	− 30%

in ozone reductions. Therefore, concurrent reduction of both NO<sub>x</sub> and VOCs during 2020 due to ongoing mitigation plan and new stringent control measures for 2020 introduced by the Chinese Ministry of Environment

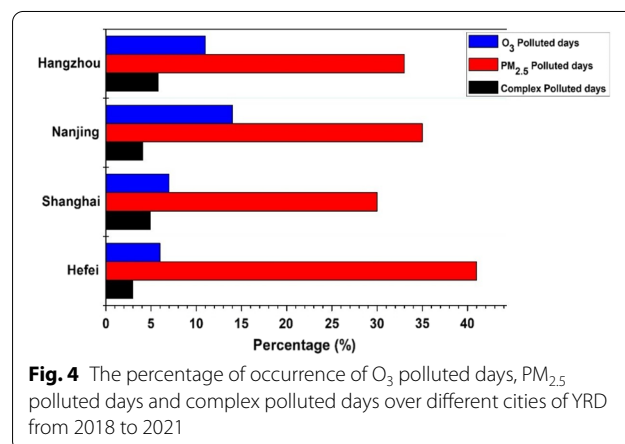


**Fig. 4** The percentage of occurrence of O<sub>3</sub> polluted days, PM<sub>2.5</sub> polluted days and complex polluted days over different cities of YRD from 2018 to 2021

and Ecology in 2020 [46] may be helped in the reduction of ozone level. However, the MDA8 O<sub>3</sub> levels again showed a slight increase during 2021 compared to 2020 over Hefei, Nanjing, and Hangzhou; whereas, Shanghai showed a continuous reduction in MDA8 O<sub>3</sub> concentration. Therefore, it is still not clear which specific measures have helped in the reduction of O<sub>3</sub> and requires further studies over different parts of China.

The daily average concentrations of PM<sub>10</sub> and PM<sub>2.5</sub> from 2018 to 2021 were used to analyze the ratio of PM<sub>2.5</sub> to PM<sub>10</sub> (PM<sub>2.5</sub>/PM<sub>10</sub>) to assess PM pollution over the studied cities (Shanghai, Nanjing, Hefei, and Hangzhou). Domestic heating and lower temperatures contributed to high PM<sub>2.5</sub>/PM<sub>10</sub> values and their rate of change during winters in general. Due to high penetration rates and enhanced diffusion, smaller particles are more harmful compared to large particles. Therefore, it is imperative to reduce the proportion of PM<sub>2.5</sub> in PM<sub>10</sub> by applying control strategies especially focusing on the reduction by vehicular discharge and industrial emissions which mainly contribute to PM<sub>2.5</sub>. Domestic heating, traffic, spatial location, and meteorology should be simultaneously considered while conducting the measures to

reduce PM pollution. The larger PM<sub>2.5</sub>/PM<sub>10</sub> are observed in Shanghai and Hefei. This is an indication that fine particulate matter from anthropogenic sources mainly influences the air quality of Hefei and Shanghai.

It is worth discussing here that COVID-19 lockdown also played a significant part in the decline of the annual mean concentration of trace gases and particulate matter during 2020. Several studies reported the impact of COVID-19 lockdown on the concentration of trace gases and particulate matter over the YRD region [47–49]. Therefore, the annual time-series of particulate matter and other trace gases were also generated excluding the COVID-19 lockdown period (i.e., 24th of January–31st of March) from each year (Additional file 1: Figure S1). The results depict that the fewer decline in annual mean concentration during 2020 is observed in time-series excluding lockdown period as compared to time-series including the COVID-19 lockdown period. Additional file 1: Table S7 shows the change in percentage of annual mean concentrations from 2019 to 2020 for whole year and excluding COVID-19 lockdown period. The results indicate that for both whole year and excluding COVID-19 lockdown period the change in percentage of trace

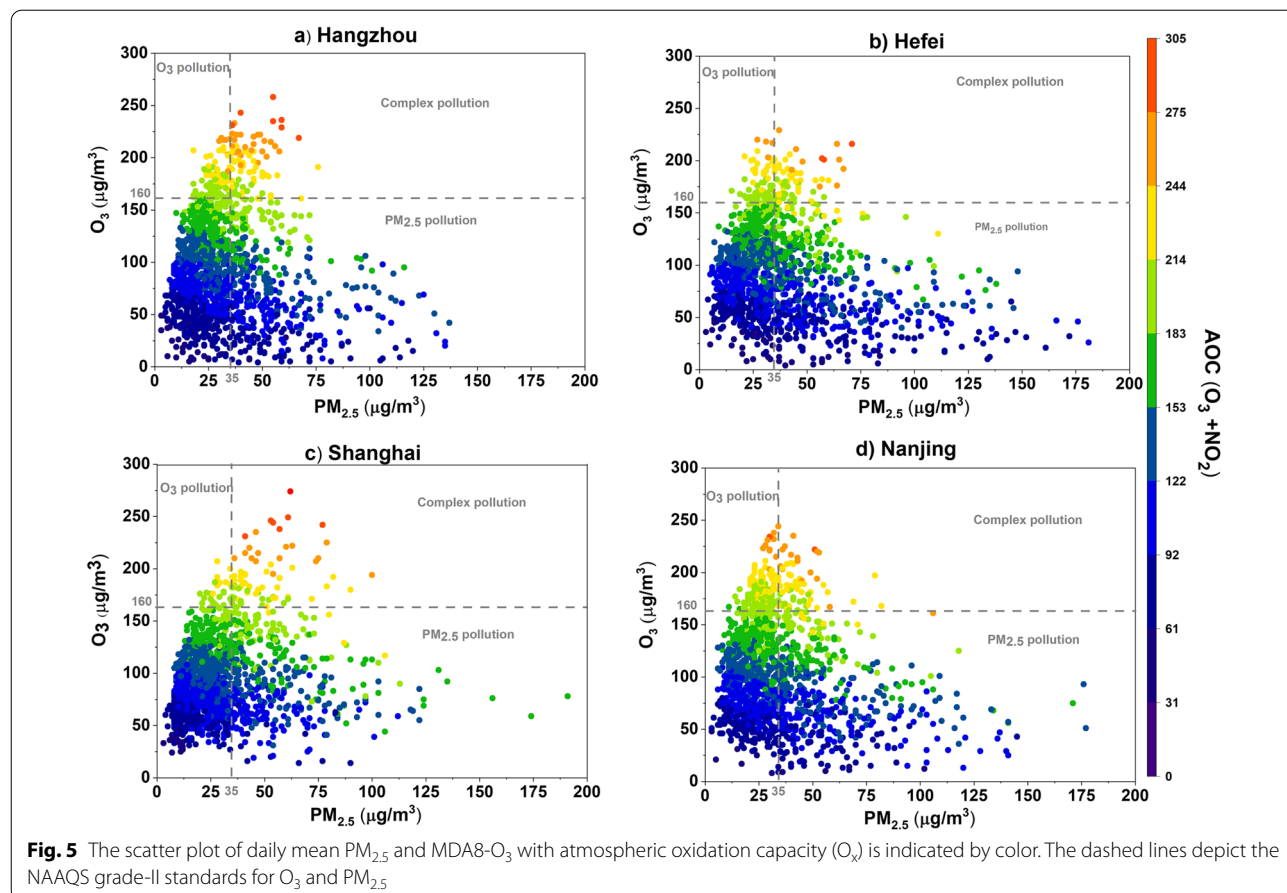
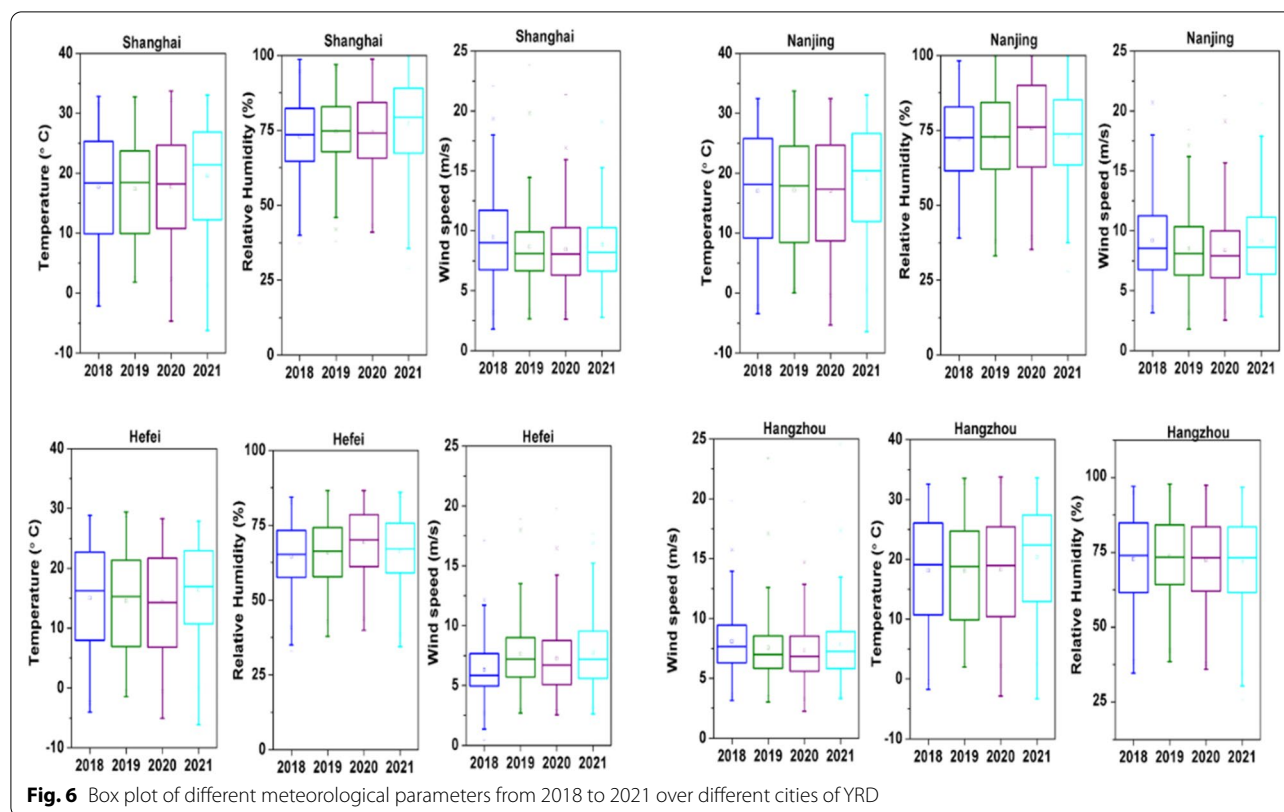


**Fig. 5** The scatter plot of daily mean PM<sub>2.5</sub> and MDA8-O<sub>3</sub> with atmospheric oxidation capacity (O<sub>x</sub>) is indicated by color. The dashed lines depict the NAAQS grade-II standards for O<sub>3</sub> and PM<sub>2.5</sub>



gases and particulate matter is negative, i.e., decline in concentration is observed. However, the results indicate that decline in concentration of NO<sub>2</sub>, SO<sub>2</sub>, PM<sub>2.5</sub> and PM<sub>10</sub> is relatively less when COVID-19 lockdown period is excluded. This shows the importance of COVID-19 lockdown which resulted in improvement of air quality. Contrasting results were noticed for O<sub>3</sub> which showed higher decline in concentration when COVID-19 lockdown period is excluded. The previous study over Nanjing also showed increase in concentration of O<sub>3</sub> during COVID-19 lockdown period [47].

**Haze pollution**

Haze formation is one of the phenomena that is largely impacted by the meteorological conditions of the locality. This haze impacts pollutants distribution, residence-time and photochemical reactions, thereby altering the atmospheric composition and impacting air quality [50, 51]. The study period is categorized into haze and non-haze days according to the categorization described above in the methodology section. Fig. 3 shows the number of haze days for all the four cities studied during the four consecutive years. Evidently, Hefei and Nanjing have the highest number of haze days, while Shanghai and Hangzhou have considerably fewer haze days compared to

other cities. However, the general trend shows an average drop in haze days occurrence from 2018 to 2021.

Further, the impact of the haze condition on the concentration of trace gases and particulate matter is also examined. Table 1 depicts the percent change in mean concentrations of NO<sub>2</sub>, SO<sub>2</sub>, O<sub>3</sub>, PM<sub>2.5</sub>, and PM<sub>10</sub> during haze days.

The concentration of all the particulate matter and trace gases except O<sub>3</sub> is higher during during haze days. This increase in concentration is mainly because meteorological conditions like low wind speed and high relative humidity were noted during haze days, which were favorable to the accumulation of air pollutants [52]. However, O<sub>3</sub> concentrations tend to be higher during non-haze days compared to haze days over all the cities. During haze days, the light intensity is low and the conditions are less likely to favor photochemical reaction, hence the rate of O<sub>3</sub> formation is low compared to non-haze sky conditions when ample sunlight is available [53]. The highest change is observed in the concentration of PM<sub>2.5</sub>.

**Complex pollution episodes**

The higher concentrations of O<sub>3</sub> and PM<sub>2.5</sub> have adversative effects on community health and the

**Table 2** Pearson correlation coefficient between air pollutants and meteorological factors (2018–2021)

Pollutant	Temperature[°C]				Relative humidity [%]				Wind speed [m/s]			
	Spring	Summer	Winter	Autumn	Spring	Summer	Winter	Autumn	Spring	Summer	Winter	Autumn
Shanghai												
PM <sub>2.5</sub>	0.110	-0.110	-0.084	-0.225	-0.003	-0.159	-0.115	0.005	-0.242	-0.450	-0.218	-0.264
PM <sub>10</sub>	0.171	0.299	-0.191	-0.146	-0.403	-0.511	-0.415	-0.260	-0.125	-0.220	-0.174	-0.258
NO <sub>2</sub>	-0.013	-0.224	0.031	-0.346	-0.063	0.097	-0.086	0.083	-0.439	-0.675	-0.429	-0.575
SO <sub>2</sub>	0.251	0.116	-0.327	-0.032	-0.307	-0.548	-0.458	-0.313	-0.107	-0.042	-0.145	-0.211
O <sub>3</sub>	0.551	0.162	0.226	0.365	-0.550	-0.525	-0.173	-0.425	-0.005	-0.283	0.069	-0.164
Hefei												
PM <sub>2.5</sub>	-0.138	0.071	0.02	-0.211	0.059	-0.330	0.13	-0.047	-0.068	-0.311	-0.25	-0.224
PM <sub>10</sub>	0.138	0.336	0.09	-0.028	-0.472	-0.635	-0.27	-0.427	-0.051	-0.266	-0.26	-0.302
NO <sub>2</sub>	0.037	-0.070	0.02	-0.260	-0.382	-0.245	-0.23	-0.333	-0.298	-0.524	-0.38	-0.547
SO <sub>2</sub>	0.117	0.248	0.04	-0.049	-0.512	-0.475	-0.59	-0.464	-0.070	-0.059	-0.24	-0.248
O <sub>3</sub>	0.652	0.266	0.19	0.692	-0.590	-0.744	-0.43	-0.463	-0.177	-0.224	0.19	-0.176
Nanjing												
PM <sub>2.5</sub>	0.05	-0.006	0.002	-0.23	0.02	-0.20	0.05	0.01	-0.19	-0.20	-0.25	-0.12
PM <sub>10</sub>	0.43	0.15	0.016	-0.19	-0.32	-0.46	-0.17	-0.34	-0.21	-0.15	-0.23	0.02
NO <sub>2</sub>	0.19	-0.03	0.071	-0.28	-0.33	-0.11	-0.13	-0.31	-0.36	-0.45	-0.40	-0.33
SO <sub>2</sub>	0.0016	0.25	-0.08	0.12	-0.40	-0.60	-0.41	-0.45	-0.32	-0.05	-0.22	-0.20
O <sub>3</sub>	0.26	0.26	0.17	0.67	-0.61	-0.70	-0.43	-0.42	-0.08	-0.09	0.17	-0.05
Hangzhou												
PM <sub>2.5</sub>	0.056	0.003	-0.015	-0.022	-0.110	-0.154	-0.093	-0.097	-0.165	-0.349	-0.246	-0.39
PM <sub>10</sub>	0.108	0.112	0.078	-0.048	-0.375	-0.295	-0.242	-0.290	-0.134	-0.284	-0.228	-0.40
NO <sub>2</sub>	-0.013	-0.382	0.076	-0.269	-0.091	0.252	-0.021	-0.106	-0.340	-0.587	-0.264	-0.57
SO <sub>2</sub>	0.078	0.160	-0.306	-0.053	-0.454	-0.420	-0.239	-0.368	-0.032	0.080	-0.074	-0.27
O <sub>3</sub>	0.554	0.302	0.146	0.633	-0.690	-0.567	-0.487	-0.622	-0.011	-0.174	0.076	-0.08

environment [14, 54]. The complex pollution episode is basically the co-occurrence of both PM<sub>2.5</sub> and MDA8 O<sub>3</sub> at higher levels. The complex pollution episodes are identified in the study period according to the categorization described in the methodology section. Fig. 4 shows the percentage of occurrence of O<sub>3</sub> polluted days (O<sub>3</sub> > 160 µg/m<sup>3</sup>), PM<sub>2.5</sub> polluted days (PM<sub>2.5</sub> > 35 µg/m<sup>3</sup>) and complex polluted days (O<sub>3</sub> > 160 µg/m<sup>3</sup> and PM<sub>2.5</sub> > 35 µg/m<sup>3</sup>) over Shanghai, Nanjing, Hefei and Hangzhou.

The results show that the highest number of PM<sub>2.5</sub> polluted days is observed in Hefei (41%), whereas the O<sub>3</sub> and complex polluted days are lowest in Hefei. The highest percentage of O<sub>3</sub> polluted days (14%) occurred in Nanjing compared to other cities. However, the highest percentage of complex polluted days occurred in Hangzhou (5.8%) and Shanghai (5%), compared to Hefei (3%) and Nanjing (4%). The primary pollutants concentration (NO<sub>2</sub> and SO<sub>2</sub>) is lower in Hangzhou and Shanghai as depicted in the previous section but the percentage of complex pollution days is higher. This is an indication that despite a reduction of primary pollutants in the main cities of China, the formation of the secondary pollutant is still a concern. During the complex pollution,

days mean O<sub>x</sub> (O<sub>3</sub>+NO<sub>2</sub>) is compared for different cities, which is an indicator of atmospheric oxidation capacity. The mean O<sub>x</sub> levels (atmospheric oxidation capacity) during complex pollution episodes indicate that Hangzhou and Shanghai have higher oxidation capacity during complex pollution days compared to Nanjing and Hefei as shown in scatter plot of daily mean PM<sub>2.5</sub> and MDA8-O<sub>3</sub> with atmospheric oxidation capacity (O<sub>x</sub>) in Fig. 5. It is pertinent to mention that PM<sub>10</sub> and MDA8-O<sub>3</sub> are also closely linked but this study mainly focused on complex pollution episodes, i.e., the co-occurrence of both PM<sub>2.5</sub> and MDA8 O<sub>3</sub> at higher levels, therefore, the scatter plots of daily mean PM<sub>2.5</sub> and MDA8-O<sub>3</sub> are presented in this study. The higher oxidation capacity can enhance the rate of secondary pollution formation. Similar results were reported in previous studies conducted in China [52].

**Influence of meteorology**

Meteorological factors play a key role in trace gas and aerosol distribution in the atmosphere and substantial pieces of evidence can be found in the literature pertaining to the impact of meteorology on local air quality [55]. Therefore, inter-annual variation in different meteorological parameters like temperature, relative humidity, and wind speed is

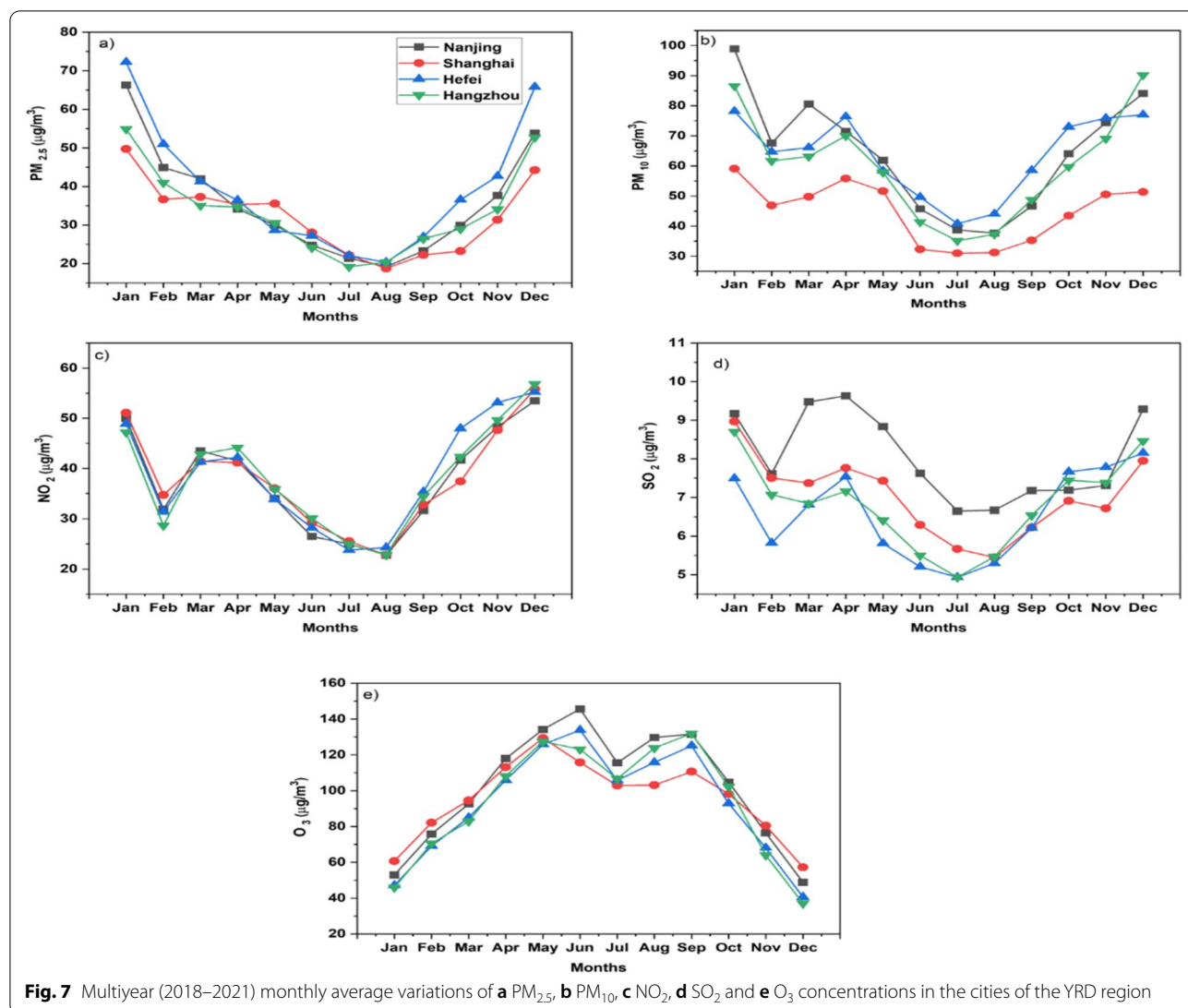


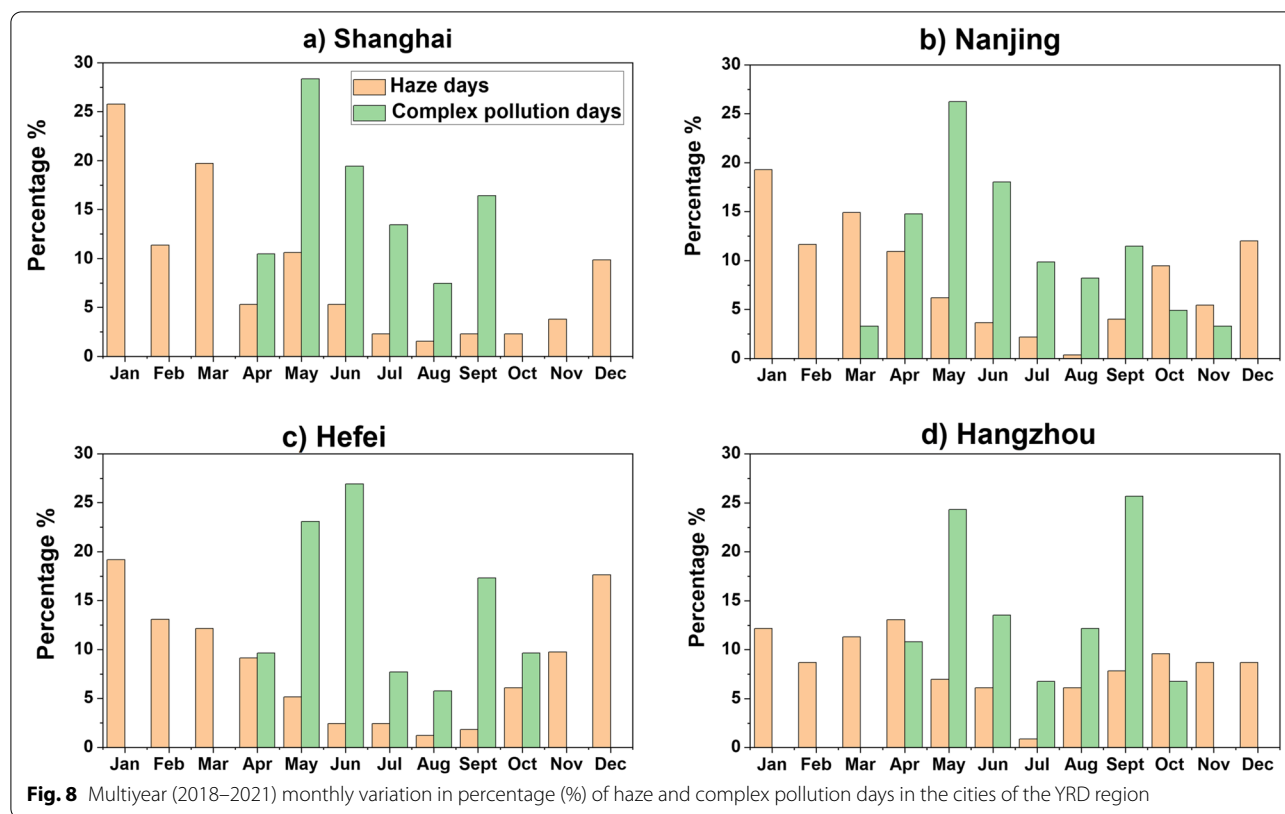
**Fig. 7** Multiyear (2018–2021) monthly average variations of **a**  $PM_{2.5}$ , **b**  $PM_{10}$ , **c**  $NO_2$ , **d**  $SO_2$  and **e**  $O_3$  concentrations in the cities of the YRD region

observed. Fig. 6 shows box plots of meteorological parameters from 2018 to 2021. The results show that there is no significant change in inter-annual variation of temperature, relative humidity, and wind speed. The meteorological conditions are almost identical from 2018 to 2021 over YRD region cities. This provided limited assurance that the air quality trends are not partially influenced by year-to-year meteorological differences. Therefore, inter-annual variations in trace gases and particulate matter are possibly due to changes in emission sources and strict measures taken by the Chinese Government.

However, the meteorological conditions at the sub-seasonal scale of a locality are considered to be a major driving force towards the distribution of pollutants in terms of residence-time and chemical behavior in the lower atmosphere. Therefore, the pairwise correlation analysis at a seasonal

scale was used to understand the relationship among meteorological factors and five criteria pollutants ( $NO_2$ ,  $SO_2$ ,  $O_3$ ,  $PM_{2.5}$ , and  $PM_{10}$ ). The correlation coefficients between pollutants and meteorological factors are depicted in Table 2. Strong negative correlation of wind speed was observed with  $NO_2$ , especially during summer and winters, compared to other parameters. The wind speed is negatively correlated with primary pollutants because lower wind speeds result in the accumulation of different primary pollutants [55]. The secondary pollutant  $O_3$  is also weakly and negatively correlated with wind speed except in the autumn season. The trend is similar over all the cities.

Temperature is positively correlated with  $O_3$  over all the cities with different values of coefficient. This correlation is relatively stronger in the spring and autumn seasons. Similar results were reported in previous studies [10, 56].



The rate of formation of O<sub>3</sub> is higher when temperature increases, as photolytic activity is increased which helps in the formation of secondary pollutant O<sub>3</sub> [11, 57]. The correlation among PM<sub>2.5</sub> levels and temperature showed a weak negative trend during the autumn season over all the cities. However, the correlations are non-significant during other seasons. The PM<sub>10</sub> levels showed a positive correlation with temperature during the spring and summer seasons, with the highest correlation ( $R = 0.43$ ) found in Nanjing during the spring season. The mean NO<sub>2</sub> levels showed weak negative correlations with temperature during the summer and autumn seasons over all the cities; whereas, the mean SO<sub>2</sub> levels showed weak negative correlations with temperature during the winter and autumn season, and weak positive correlations during the spring and summer seasons. The relative humidity is negatively correlated with all the pollutants. The concentration of O<sub>3</sub> showed a strong negative correlation with relative humidity. The NO<sub>2</sub> and PM<sub>2.5</sub> are weakly and negatively correlated with relative humidity. However, SO<sub>2</sub> and PM<sub>10</sub> are found to be moderate and negatively correlated. A similar trend is observed over all the cities.

Generally, the impact of the meteorological parameters on pollutant concentration is similar over all the cities of YRD. The increase in temperature and lower relative

humidity favors the accumulation of O<sub>3</sub>, while low temperature, low wind speeds, and lower relative humidity favor the accumulation of primary pollutants.

### Monthly variations

The monthly variations in air pollutants over Shanghai, Nanjing, Hefei, and Hangzhou are investigated. Fig. 7 depicts multiyear (2018–2021) monthly variations in five criteria pollutants over the four cities. The results indicated that the pollutant concentrations are higher during the winter months for all the species (except O<sub>3</sub>). The concentration of pollutants began to rise in September and peaks were found in December–January. The peak values were observed during January for PM<sub>2.5</sub> and PM<sub>10</sub> except for Hangzhou where PM<sub>10</sub> peaked during December. NO<sub>2</sub> concentration peaked in December for all the cities while SO<sub>2</sub> remained highest during January for Shanghai and Hangzhou, while for Nanjing and Hefei, it peaked during December. In contrast, O<sub>3</sub> concentrations were observed to rise during the summer months with the highest value occurring in the May–June months.

The concentration of particulate matter peaked during the winter season due to different reasons. These reasons include stagnant meteorological conditions [lower temperature, lower wind speed] of locality [12], higher coal combustion for the heating purpose [58, 59], and

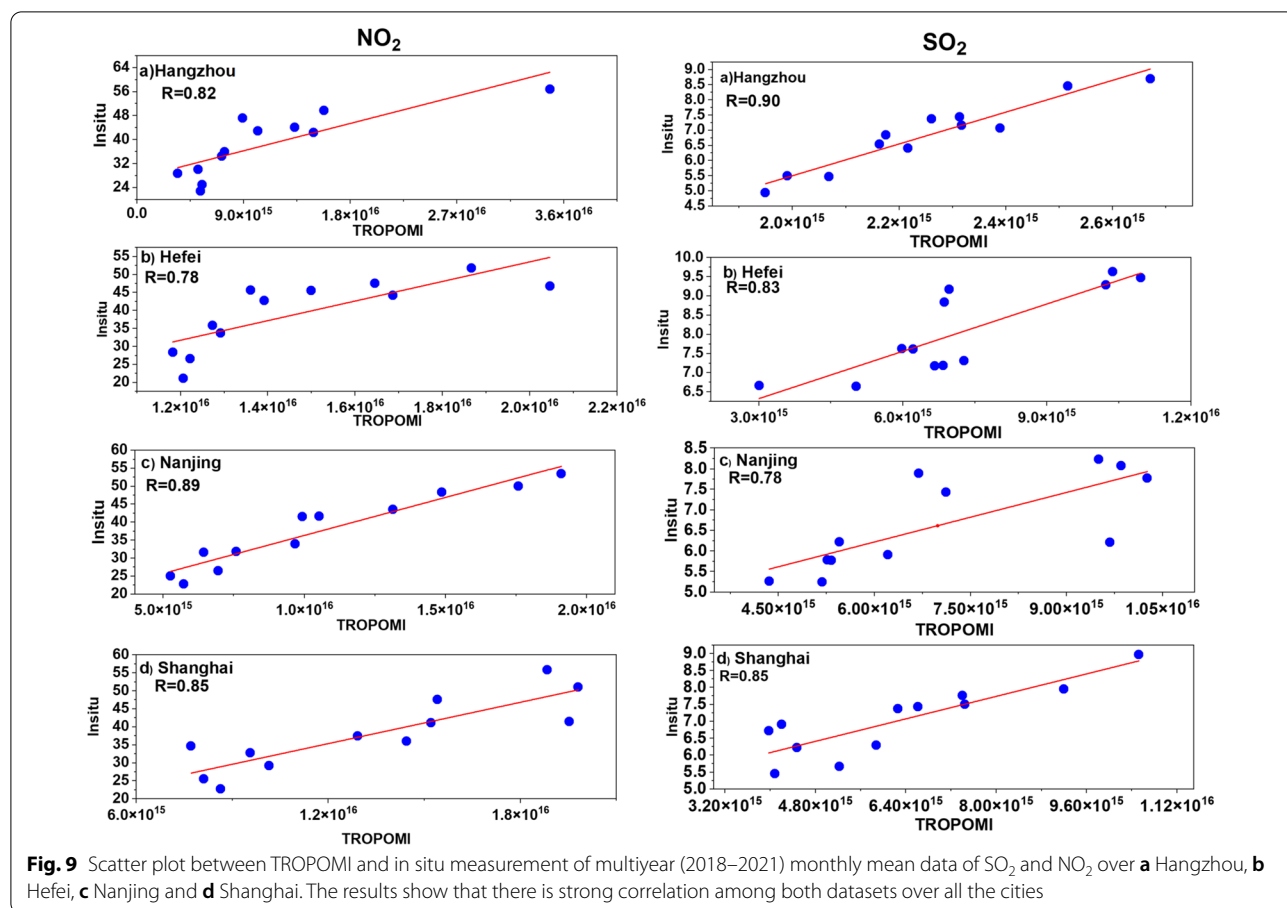


**Table 3** Factor loadings after PCA analysis Varimax rotation

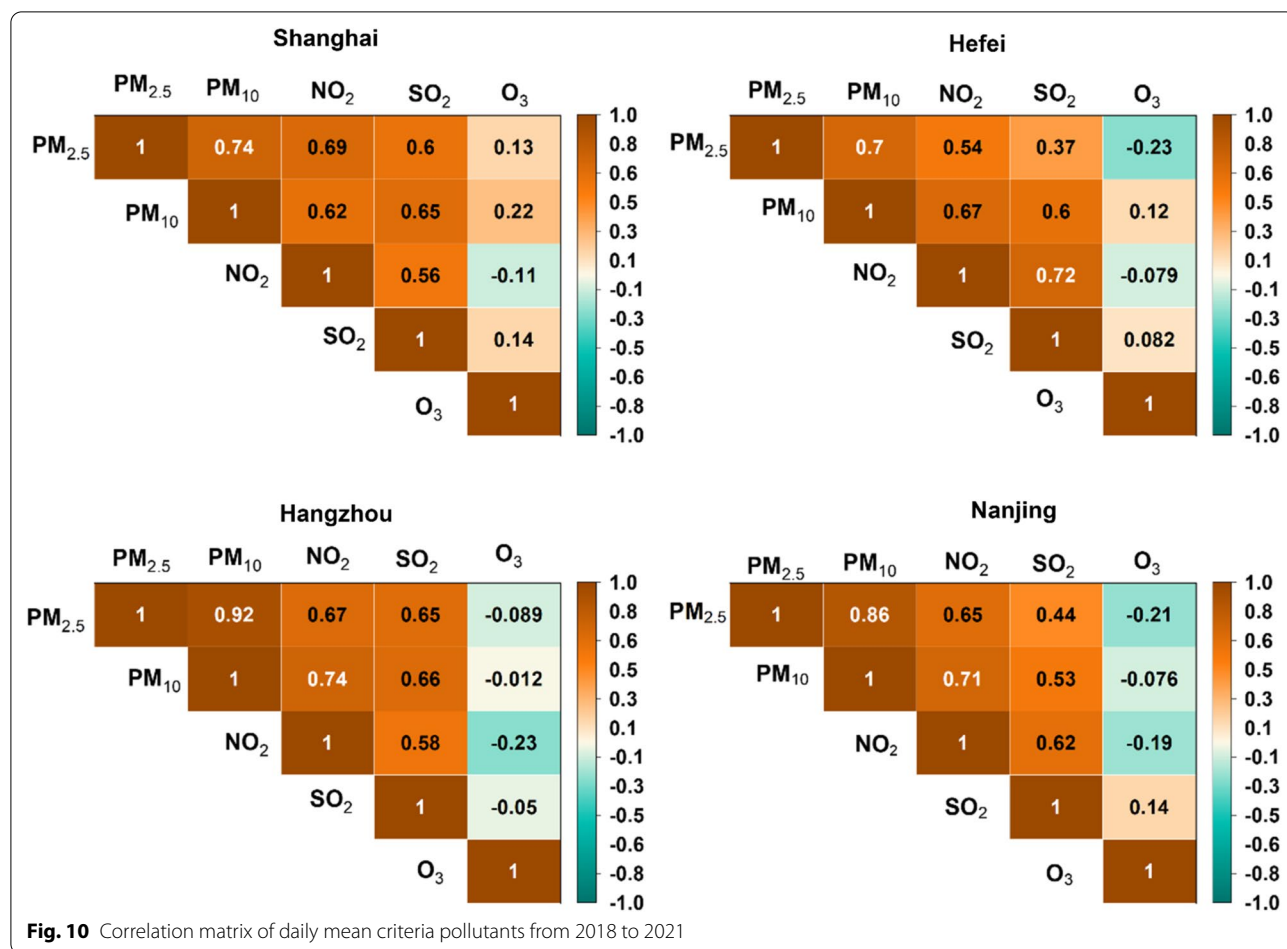
	Hefei		Nanjing		Shanghai		Hangzhou	
	Factor 1	Factor 2	Factor 1	Factor 2	Factor 1	Factor 2	Factor 1	Factor 2
PM <sub>2.5</sub>	0.744		PM <sub>2.5</sub>	0.867	PM <sub>2.5</sub>	0.886	PM <sub>2.5</sub>	0.926
PM <sub>10</sub>	0.899		PM <sub>10</sub>	0.916	PM <sub>10</sub>	0.869	PM <sub>10</sub>	0.954
SO <sub>2</sub>	0.819		SO <sub>2</sub>	0.756	SO <sub>2</sub>	0.854	SO <sub>2</sub>	0.814
NO <sub>2</sub>	0.879		NO <sub>2</sub>	0.873	NO <sub>2</sub>	0.806	NO <sub>2</sub>	0.825
O <sub>3</sub>		0.961	O <sub>3</sub>		0.953	O <sub>3</sub>		0.978
								0.990

formation of new particles and secondary organic–inorganic aerosols [12, 60]. Similarly, the concentration of SO<sub>2</sub> and NO<sub>2</sub> is also higher during winter months due to increased burning of biomass fuel coupled with reduced air temperature, wind speed, and solar radiations [36].

However, the concentration of O<sub>3</sub> is higher in the summer months which can be attributed to the fact that photochemical reactions are its precursors. The monthly mean variation in the O<sub>3</sub> levels shows an M-shaped curve, and the O<sub>3</sub> peaks were observed in May and September

for Shanghai and Hangzhou; whereas, in Hefei and Nanjing, the O<sub>3</sub> peaks were observed in June and September. Similar monthly variations of O<sub>3</sub> were reported in a study over south China [61]. The monthly variations of pollutants are consistent with findings of previous studies over different cities of China [12, 62].

There are a few anomalies in the results which are worth mentioning. The concentration of NO<sub>2</sub>, SO<sub>2</sub>, and PM<sub>10</sub> showed a sudden decline in February. This can be linked to the fact that the Spring festival which is the



most valuable vacation for Chinese people occurred in February during these years (Additional file 1: Table S8). The majority of migrant residents of megacities return to their hometowns. The closure of industries, offices, and educational institutes is observed over all the regions of China during the spring festival. Therefore, the reduction in anthropogenic activities results in a sudden dip in pollutants concentrations. Similar results were reported in previous studies explaining the impact of the spring festival on pollutants concentration [48, 53].

Fig. 8 shows the percentage of haze and complex pollution days occurrence in different months from 2018 to 2021. It is observed that complex pollution days mainly occurred in summer, whereas the higher percentage of haze days occurred in winter. The maximum haze days occurred in January over all the cities. This occurrence of haze episodes in winter months can be attributed to the fact that fine particulates concentration is higher in winter which plays an important role in haze formation; whereas, the maximum complex pollution days occurred in May over Shanghai and Nanjing, in June over Hefei, and in September over Hangzhou. This distribution of

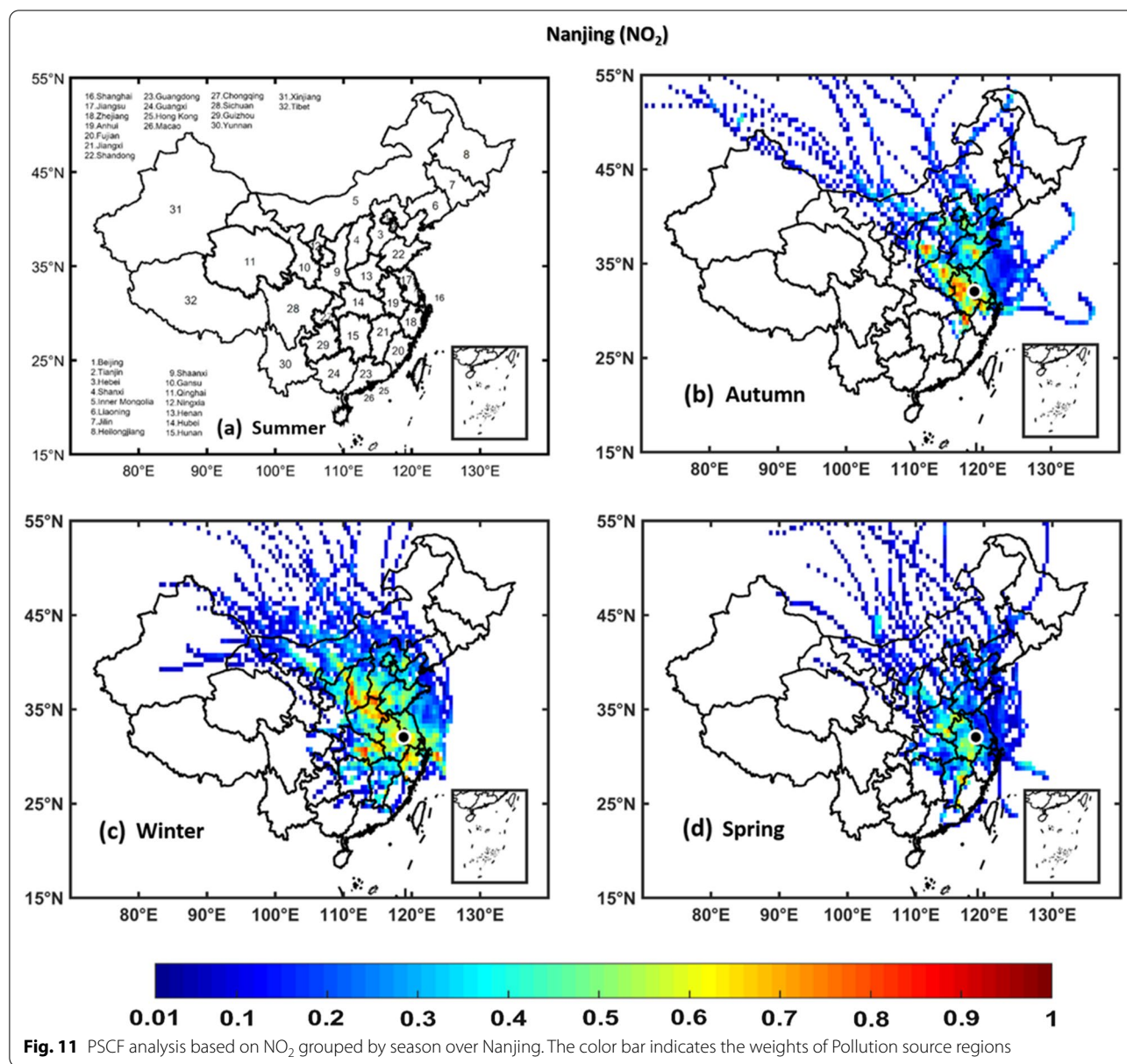
complex days is mainly because O<sub>3</sub> and PM<sub>2.5</sub> are negatively correlated during winter and autumn. However, the correlation is moderate positive during late spring and summer [63, 64].

**TROPOMI validation**

The in situ measurements for trace gases including SO<sub>2</sub> and NO<sub>2</sub> are compared with spatially averaged TROPOMI satellite data of SO<sub>2</sub> and NO<sub>2</sub> over different cities of YRD region. The multiyear (2018–2021) monthly mean values of SO<sub>2</sub> and NO<sub>2</sub> are compared with each other. Fig. 9 shows correlation plot among in situ and TROPOMI satellite data.

**Principal component analysis and correlation analysis**

PCA was used to reveal possible sources of pollutants emissions and calculate correlations between them. PCA is a frequently utilized multi-variate statistical analysis tool that is crucial to the study of interrelationships between diverse variables coming from a similar transference path or source [12, 33]. Additional file 1: Tables

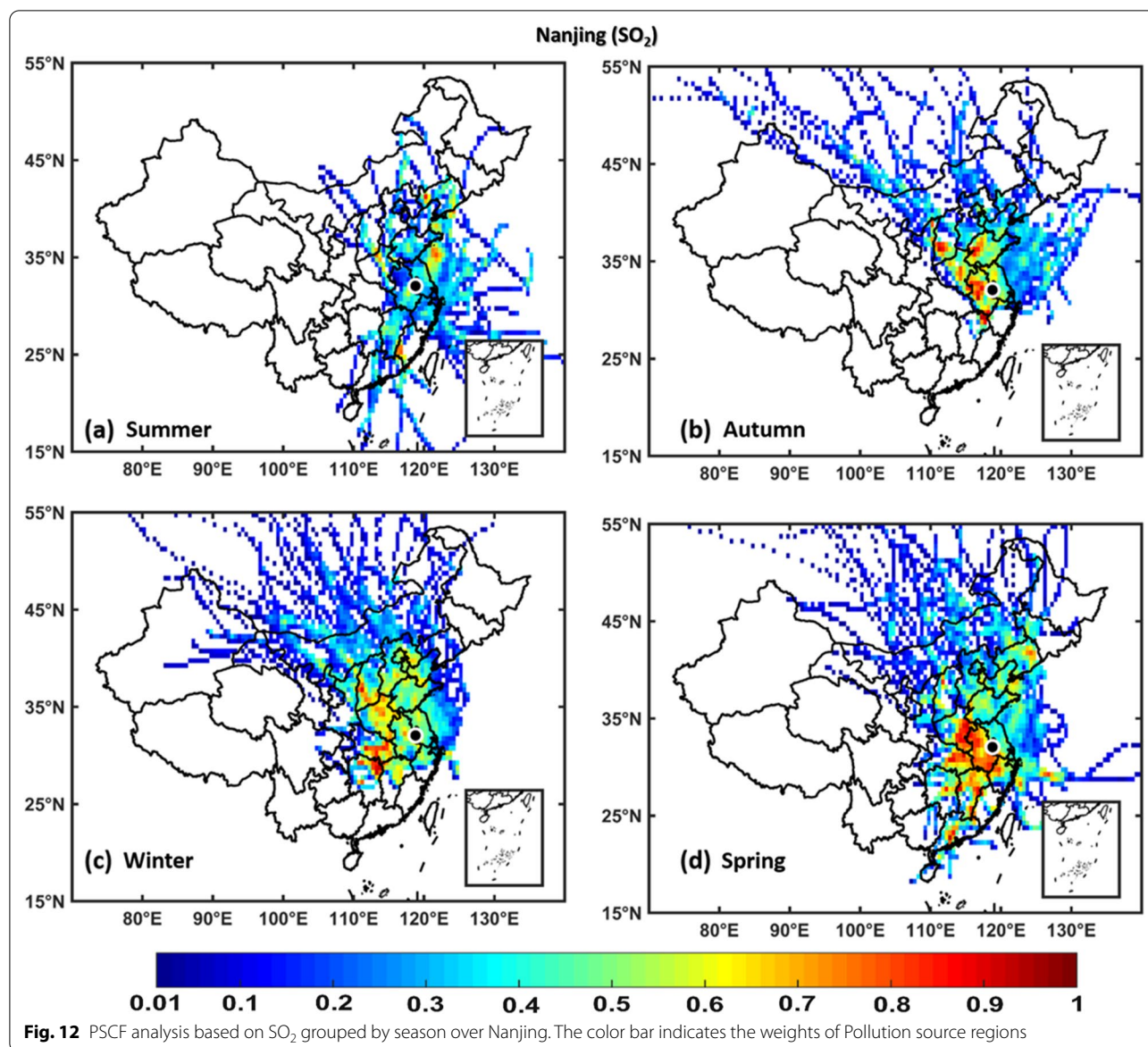


S9–S12 represents the total variance and rotated component matrix of PCA of atmospheric pollutants concentrations in our study area. Two factors were obtained which explain 83%, 81%, 80%, and 78% total variability over Hangzhou, Shanghai, Nanjing, and Hefei. Table 3 depicts the two factors obtained through PCA.

Factor 1 has positive loading of SO<sub>2</sub>, PM<sub>2.5</sub>, PM<sub>10</sub>, and NO<sub>2</sub>. These all are indicative of primary anthropogenic sources (industrial, coal, biomass and fossil fuel). However, factor 2 has positive loading of O<sub>3</sub> reflecting markedly unlike sources that are photochemical reactions. Similar results were observed over all the cities with different values. These results are consistent with findings

over urban cities of Lanzhou, Urumqi, Jinan and Shanghai [12, 33, 65, 66]. It is worth mentioning that Lanzhou, Urumqi and Jinan are located at geographically different locations as compared to study area. Fig.10 depicts the correlation matrix of trace gases and particulate matter over cities of the YRD region.

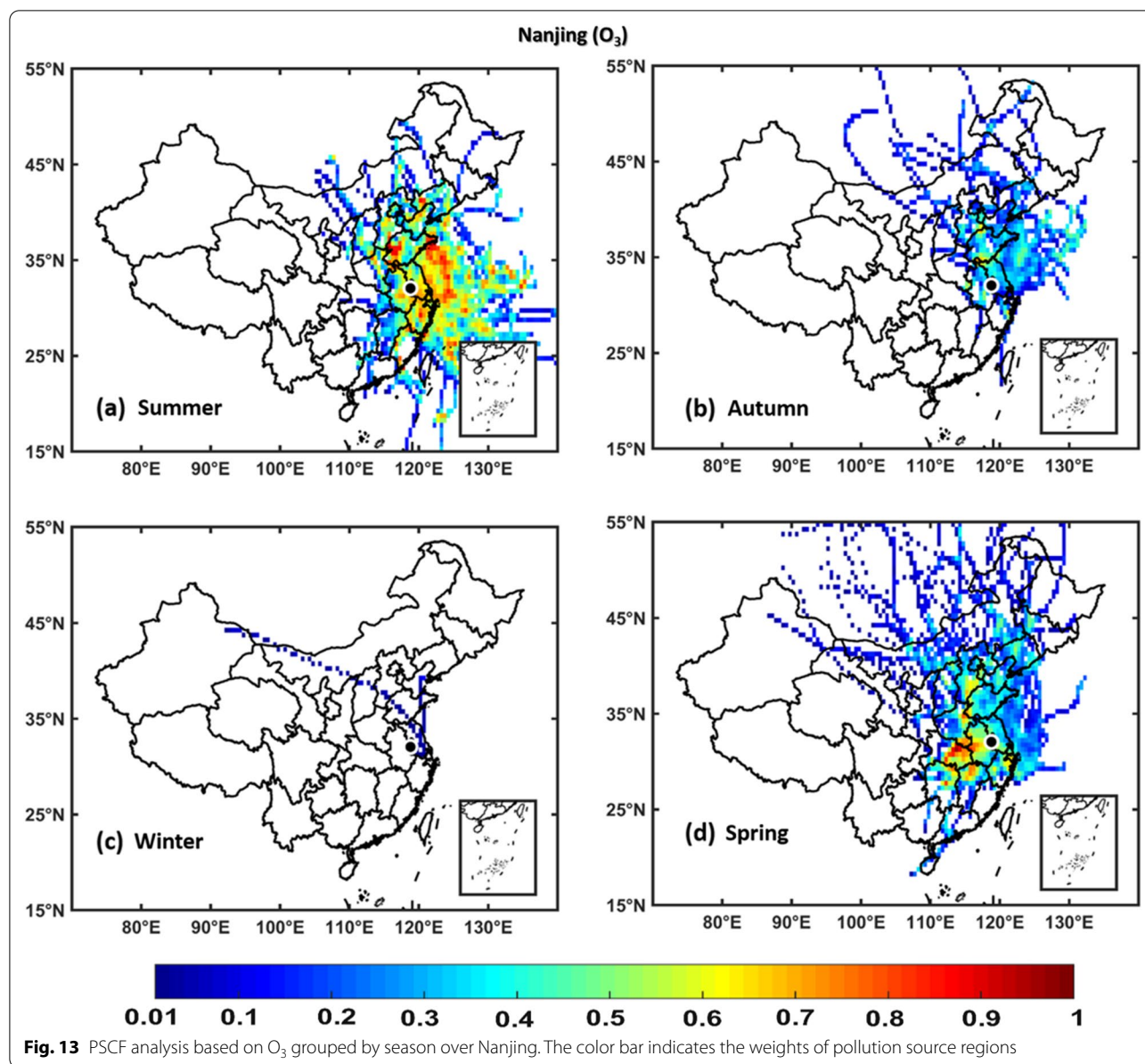
The daily mean PM<sub>2.5</sub> concentrations are strongly correlated with daily mean PM<sub>10</sub> concentration in all the cities. The strongest correlation is observed over Hangzhou as compared to other cities. Particulate matter (PM<sub>2.5</sub> and PM<sub>10</sub>) shows an almost similar correlation trend with NO<sub>2</sub> and SO<sub>2</sub> over all the cities of the study. The positive correlation between particulate



matter (PM<sub>2.5</sub> and PM<sub>10</sub>) with SO<sub>2</sub> and NO<sub>2</sub> is noted. This indicates that particulate matters (PM<sub>2.5</sub> and PM<sub>10</sub>), and primary trace gases (SO<sub>2</sub> and NO<sub>2</sub>) have similar sources of emissions like fossil fuel combustion and traffic. The recent studies also stated a strong positive correlation between particulate matters (PM<sub>2.5</sub> and PM<sub>10</sub>), and primary trace gases in Beijing [67] and Delhi [68]. The correlation of O<sub>3</sub> with other trace gases and particulate matter showed diverse trends over the different cities of this study. A weak positive correlation is observed between particulate matter (PM<sub>2.5</sub> and PM<sub>10</sub>) and O<sub>3</sub> over Shanghai; whereas, over Hangzhou

and Nanjing this correlation among is particulate matters (PM<sub>2.5</sub> and PM<sub>10</sub>) and O<sub>3</sub> weak negative. PM<sub>2.5</sub> is negatively correlated with O<sub>3</sub> in Hefei, whereas PM<sub>10</sub> showed a weak positive correlation. A weak negative correlation is observed among NO<sub>2</sub> over all the cities. The correlation coefficient between SO<sub>2</sub> and O<sub>3</sub> is weak positive over Shanghai and Nanjing; whereas, the correlation coefficient between SO<sub>2</sub> and O<sub>3</sub> is weak negative over Hefei and Hangzhou.

The results depict that O<sub>3</sub> had distinctly different sources as compared to primary trace gases and particulate matters. The negative correlation of O<sub>3</sub> with NO<sub>2</sub> can be explained by studying the tropospheric chemistry where



the reaction of O<sub>3</sub> with NO leads to the formation of NO<sub>2</sub> thereby depleting O<sub>3</sub> [69]. These results comply with previously reported findings [10, 55].

**Potential source contribution function**

PSCF analyses were performed to identify the potential source areas of NO<sub>2</sub>, SO<sub>2</sub>, O<sub>3</sub>, PM<sub>2.5</sub>, and PM<sub>10</sub> over Hangzhou, Hefei, Nanjing, and Shanghai regions using seasonal in situ measurements of NO<sub>2</sub>, SO<sub>2</sub>, O<sub>3</sub>, PM<sub>2.5</sub>, and PM<sub>10</sub> as input in the PSCF model and 72-h back trajectories obtained from the NOAA HYSPLIT model. The regions with WPSCF less than 0.4 are described as low pollution source, regions with WPSCF ranging

from 0.4-0.5 are described as medium pollution source, whereas areas with WPSCF greater than 0.5 are termed as high pollution source regions. The results show that the air quality over Hangzhou, and Hefei, Nanjing, and Shanghai are significantly affected by local [neighboring provinces and cities within China] pollution sources of NO<sub>2</sub>, SO<sub>2</sub>, PM<sub>2.5</sub>, and PM<sub>10</sub> pollutants, which are stronger in winter and weaker in summer, whereas an opposite scenario was observed for O<sub>3</sub>. Figs. 11, 12, 13, 14, 15 (Additional file 1: Figures S2–S16) show PSCF Analysis based on NO<sub>2</sub>, SO<sub>2</sub>, O<sub>3</sub>, PM<sub>2.5</sub>, and PM<sub>10</sub>, respectively grouped by season over Nanjing (Hefei, Hangzhou and Shanghai, respectively). Additional file 1:

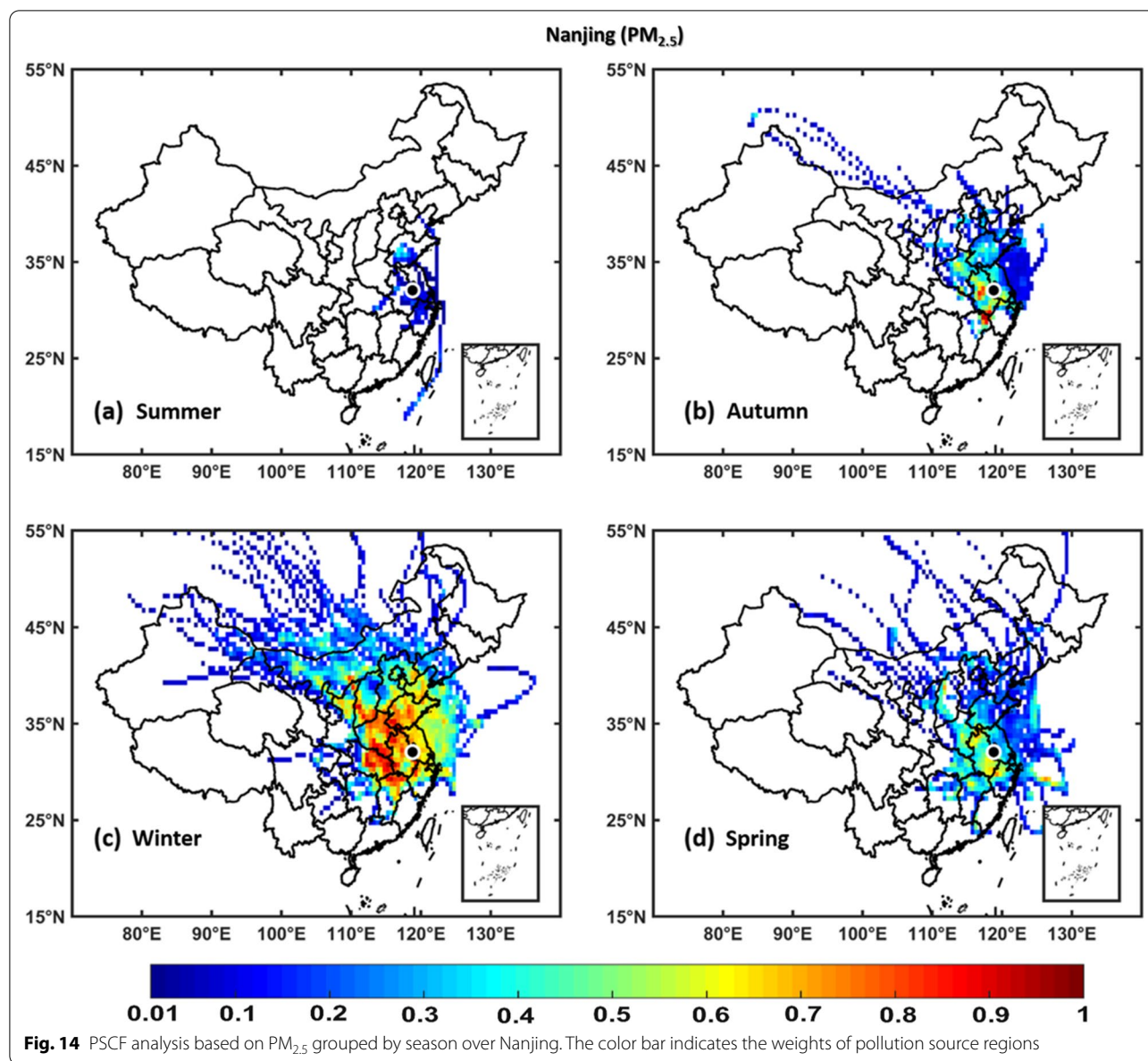
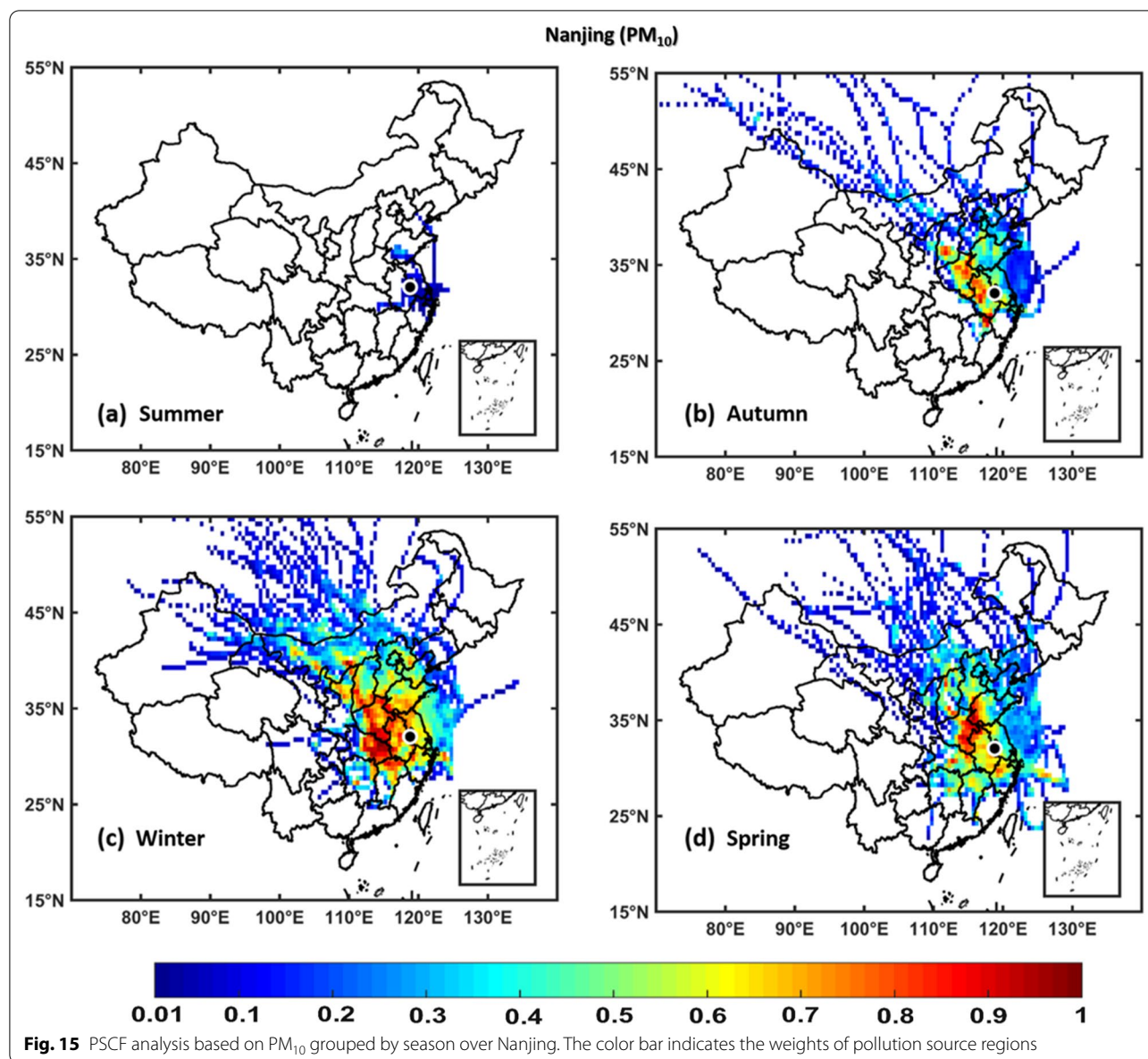


Figure S17 shows different regions in People’s republic of China Figs.12, 13, 14,15 .

Generally, the wintertime high values of PSCF (> 0.50) over Hangzhou, Hefei, Nanjing, and Shanghai regions indicate the stronger contributions from local source areas (Anhui, Beijing, Chongqing, Fujian, Hebei, Henan, Hubei, Hunan, Guangdong, Jiangsu, Jiangxi, Inner Mongolia, Shanxi, Shaanxi, Shandong, Sichuan, Tianjin, and Zhejiang). These local sources of PM<sub>2.5</sub> concentrations more significantly affect the air quality of Hangzhou, Hefei, Nanjing, and Shanghai than regional sources. In spring, the most common local source areas (e.g., Anhui, Fujian, Hebei, Henan, Hubei, Hunan, Guangdong,

Jiangsu, Jiangxi, Inner Mongolia, Shanxi, Shandong, and Zhejiang) of NO<sub>2</sub>, SO<sub>2</sub>, O<sub>3</sub>, PM<sub>2.5</sub>, and PM<sub>10</sub> concentrations also substantially affect the air quality of Hangzhou, Hefei, Nanjing, and Shanghai.

The summertime air quality of these four study areas was significantly influenced by O<sub>3</sub>, whereas the lowest contributions were noted for NO<sub>2</sub>, SO<sub>2</sub>, PM<sub>2.5</sub>, and PM<sub>10</sub> concentrations. This is showing the influence of local meteorology on aerosol pollutants and trace gases, i.e., more dispersion of aerosols and trace gases is occurred in summer than winter due to strong solar radiations, high temperatures leading to a high planetary boundary layer [36, 70]. However, the most common potential source



areas of O<sub>3</sub> concentrations are Anhui, Beijing, Fujian, Hebei, Henan, Hubei, Hunan, Guangdong, Jiangsu, Jiangxi, Shanxi, Shandong, Tianjin, and Zhejiang. In addition, the autumn air quality over Hangzhou, Hefei, Nanjing, and Shanghai are significantly impacted by local pollution sources. Overall, the results show that local sources from mainland China are the major contributors of air pollution over Hangzhou, Hefei, Nanjing, and Shanghai, with PM<sub>2.5</sub> pollution levels being higher in winter than in other seasons, whereas O<sub>3</sub> pollution is higher in summer.

### Conclusions

This study investigates the recent spatiotemporal variations (2018–2021) of trace gases and aerosols along with the impact of trans-boundary air contamination and the effect of meteorological parameters on air quality in the cities of YRD region (Shanghai, Hefei, Hangzhou and Nanjing). The annual mean concentration of NO<sub>2</sub> and PM<sub>2.5</sub> continuously declines from 2019 to 2021 over all the cities. The unprecedented decline in annual mean O<sub>3</sub> concentration is observed in 2020 over the cities of YRD region. The concurrent reduction of both NO<sub>x</sub> and VOCs during 2020 due to ongoing mitigation plan and new stringent control measures introduced by the Chinese Ministry of Environment

and Ecology in 2020 may be helped in the reduction of O<sub>3</sub> concentration. The results showed still particulate matters exceeded the NAAQS and WHO guidelines although strict measures have resulted in significant improvement of air quality. The Haze pollution events occurred more frequently in Hefei and Nanjing as compared to Shanghai and Hangzhou. This can be attributed to higher concentration of PM<sub>2.5</sub> in Hefei and Nanjing. The complex pollution episodes, i.e., the concurrent occurrence of PM<sub>2.5</sub> and O<sub>3</sub> are higher in Shanghai and Hangzhou possibly due to higher atmospheric oxidation capacity which enhances the rate of secondary pollution formation. The primary pollutants concentrations were higher in the winter, whereas O<sub>3</sub> levels were higher during the summer season. The higher concentration of trace gases and particulate matter were mainly due to trans-boundary transport from adjoining cities and provinces. The increase in temperature and lower relative humidity favors the accumulation of O<sub>3</sub>, while low temperature, low wind speeds, and lower relative humidity favor the accumulation of primary pollutants. Different cities have different pollution characteristics, requiring continuous monitoring to design city-specific policies and action plans. The results of this study can be used as a strong reference for the future research by scientific community, administration and policymakers, and other stakeholders who might be concerned about air pollution impacts and mitigation over this vast, populous and economically crucial region. Future emission control strategies should be designed considering the synchronized control of O<sub>3</sub> and PM<sub>2.5</sub>, especially for the cities with higher atmospheric oxidation capacity.

#### Abbreviations

µg/m<sup>3</sup>: Microgram per cubic meter; AGL: Above ground level; AMF: Air mass factor; DOAS: Differential optical absorption spectroscopy; FGD: Fuel gas desulfurization; GDAS: Global data assimilation system; GDP: Gross domestic product; HYSPLIT: Hybrid single-particle Lagrangian integrated trajectory; MDA8 ozone: Maximum daily 8-hour average ozone; NAAQS: National Ambient Air Quality Standards; NCP: North China Plain; NO<sub>2</sub>: Nitrogen dioxide; NOAA: National Oceanic and Atmospheric Administration; O<sub>3</sub>: Ozone; PC: Principal component; PCA: Principal component analysis; PM: Particulate matter; PSCF: Potential source contribution function; SCD: Slant column density; SO<sub>2</sub>: Sulphur dioxide; TROPOMI: Tropospheric monitoring instrument; VCD: Vertical column density; VOCs: Volatile organic compounds; WHO: World Health Organization; WPSCF: Weighted PSCF; YRD: Yangtze River Delta.

#### Supplementary Information

The online version contains supplementary material available at <https://doi.org/10.1186/s12302-022-00668-2>.

**Additional file 1: Table S1.** The spatial position of National monitoring stations over the studied cities of YRD region. **Table S2.** Criteria air pollutants in Hangzhou during the study period (2018–2021). **Table S3.** Criteria air pollutants in Nanjing during the study period (2018–2021). **Table S4.**

Criteria air pollutants in Hefei during the study period (2018–2021).

**Table S5.** Criteria air pollutants in Shanghai during the study period (2018–2021). **Table S6.** The standards for annual mean concentration (µg/m<sup>3</sup>) of different pollutants. **Table S7.** The relative (%) change in concentration of trace gases and particulate matter from 2019–2020. **Table S8.** Spring Festival during different Years in China. **Table S9.** Total variance and rotated component matrix of PCA of pollutants concentrations over Nanjing. **Table S10.** Total variance and rotated component matrix of PCA of pollutants concentrations over Hangzhou. **Table S11.** Total variance and rotated component matrix of PCA of pollutants concentrations over Shanghai. **Table S12.** Total variance and rotated component matrix of PCA of pollutants concentrations over Hefei. **Figure S1.** The inter-annual variation of NO<sub>2</sub>, O<sub>3</sub>, SO<sub>2</sub>, PM<sub>2.5</sub> and PM<sub>10</sub> in Hangzhou, Nanjing, Hefei and Shanghai during 2018–2021 excluding COVID-19 lockdown days (24th of January–31st of March) from all years. **Figure S2.** PSCF Analysis based on NO<sub>2</sub> grouped by season over Hefei. The color bar indicates the weights of Pollution source regions. **Figure S3.** PSCF Analysis based on SO<sub>2</sub> grouped by season over Hefei. The color bar indicates the weights of Pollution source regions. **Figure S4.** PSCF Analysis based on O<sub>3</sub> grouped by season over Hefei. The color bar indicates the weights of Pollution source regions. **Figure S5.** PSCF Analysis based on PM<sub>2.5</sub> grouped by season over Hefei. The color bar indicates the weights of Pollution source regions. **Figure S6.** PSCF Analysis based on PM<sub>10</sub> grouped by season over Hefei. The color bar indicates the weights of Pollution source regions. **Figure S7.** PSCF Analysis based on NO<sub>2</sub> grouped by season over Hangzhou. The color bar indicates the weights of Pollution source regions. **Figure S8.** PSCF Analysis based on SO<sub>2</sub> grouped by season over Hangzhou. The color bar indicates the weights of Pollution source regions. **Figure S9.** PSCF Analysis based on O<sub>3</sub> grouped by season over Hangzhou. The color bar indicates the weights of Pollution source regions. **Figure S10.** PSCF Analysis based on PM<sub>2.5</sub> grouped by season over Hangzhou. The color bar indicates the weights of Pollution source regions. **Figure S11.** PSCF Analysis based on PM<sub>10</sub> grouped by season over Hangzhou. The color bar indicates the weights of Pollution source regions. **Figure S12.** PSCF Analysis based on NO<sub>2</sub> grouped by season over Shanghai. The color bar indicates the weights of Pollution source regions. **Figure S13.** PSCF Analysis based on SO<sub>2</sub> grouped by season over Shanghai. The color bar indicates the weights of Pollution source regions. **Figure S14.** PSCF Analysis based on O<sub>3</sub> grouped by season over Shanghai. The color bar indicates the weights of Pollution source regions. **Figure S15.** PSCF Analysis based on PM<sub>2.5</sub> grouped by season over Shanghai. The color bar indicates the weights of Pollution source regions. **Figure S16.** PSCF Analysis based on PM<sub>10</sub> grouped by season over Shanghai. The color bar indicates the weights of Pollution source regions. **Figure S17.** Different regions of Peoples republic of China.

#### Acknowledgements

All authors are highly obliged towards China National Environmental Monitoring Center for Providing the datasets used in this study. The authors also acknowledge the the NOAA Air Resources Laboratory (ARL) for the provision of the HYSPLIT air parcel back trajectories (<https://www.ready.noaa.gov>) used in this publication.

#### Author contributions

ZJ: conceptualization, methodology, formal analysis, data curation, visualization, writing—original draft, writing—review and editing. XZ: conceptualization, supervision, funding acquisition, writing—review and editing. MB: writing—review and editing, supervision, data curation, conceptualization, funding acquisition. ZQ: methodology, writing—review and editing. GL: data curation, visualization. OS: formal analysis, data curation. KM: formal analysis, writing—review and editing. YW and Md. AA: data curation. CL and YW: writing—review and editing. DD: writing—review and editing, project administration. All authors read and approved the final manuscript.

#### Funding

This study was supported by the Jiangsu Funding Program for Excellent Postdoctoral Talent (Grant No. 2022ZB651), National Natural Science Foundation of China [Grant No. 32071521], the Scientific Research Foundation for Senior Talent of Jiangsu University, China [Grant No. 20JDG067], the Jiangsu Province “Double Innovation PhD” Grant, Special Project of Jiangsu Distinguished

Professor [R2018T22], and the Startup Foundation for Introduction Talent of NUIST [2017r107].

#### Availability of data and materials

The datasets used and/or analyzed during the current study are available from the corresponding author on reasonable request.

#### Declarations

#### Ethics approval and consent to participate

Not applicable.

#### Consent for publication

Availability of data and material

#### Competing interests

The authors declare no competing interests.

#### Author details

<sup>1</sup>Institute of Environment and Ecology, School of the Environment and Safety Engineering, Jiangsu University, Zhenjiang 212013, China. <sup>2</sup>School of Marine Sciences, Nanjing University of Information Science and Technology, Nanjing 210044, China. <sup>3</sup>National Agromet Center, Pakistan Meteorological Department, Islamabad 44000, Pakistan. <sup>4</sup>Key Laboratory of Meteorological Disaster, Ministry of Education [KLME]/Joint International Research Laboratory of Climate and Environment Change [ILCEC]/Collaborative Innovation Center On Forecast and Evaluation of Meteorological Disasters [CIC-FEMD]/CMA Key Laboratory for Aerosol-Cloud-Precipitation, Nanjing University of Information Science and Technology, Nanjing 210044, China. <sup>5</sup>Department of Precision Machinery and Precision Instrumentation, University of Science and Technology of China, Hefei 230026, China. <sup>6</sup>Key Laboratory of Environmental Optics & Technology, Anhui Institute of Optics and Fine Mechanics, Hefei Institutes of Physical Science, Chinese Academy of Sciences, Hefei 230031, China. <sup>7</sup>Center for Excellence in Regional Atmospheric Environment, Institute of Urban Environment, Chinese Academy of Sciences, Xiamen 361021, China. <sup>8</sup>Key Laboratory of Precision Scientific Instrumentation of Anhui Higher Education Institutes, University of Science and Technology of China, Hefei 230026, China. <sup>9</sup>School of Earth and Atmospheric Sciences, Georgia Institute of Technology, Atlanta, GA 30332, USA. <sup>10</sup>Shanghai Key Laboratory of Atmospheric Particle Pollution and Prevention [LAP3], Department of Environmental Science and Engineering, Fudan University, Shanghai 200433, China.

Received: 4 June 2022 Accepted: 21 August 2022

Published online: 08 September 2022

#### References

- Ji H, Wang J, Meng B, Cao Z, Yang T, Zhi G, Chen S, Wang S, Zhang J (2022) Research on adaption to air pollution in Chinese cities: evidence from social media-based health sensing. *Environ Res*. <https://doi.org/10.1016/j.envres.2022.112762>
- Li C, Managi S (2022) Spatial variability of the relationship between air pollution and well-being. *Sustain Cities Soc* 76:103447. <https://doi.org/10.1016/j.scs.2021.103447>
- Wang Y, Duan X, Liang T, Wang L, Wang L (2022) Analysis of spatiotemporal distribution characteristics and socioeconomic drivers of urban air quality in China. *Chemosphere* 291:132799. <https://doi.org/10.1016/j.chemosphere.2021.132799>
- Wang L, Li P, Yu S, Mehmood K, Li Z, Chang S, Liu W, Rosenfeld D, Flagan RC, Seinfeld JH (2018) Predicted impact of thermal power generation emission control measures in the Beijing-Tianjin-Hebei region on air pollution over Beijing China. *Sci Rep* 8(1):1–10. <https://doi.org/10.1038/s41598-018-19481-0>
- Seinfeld JH, Pandis SN (2016) Chapter 2: atmospheric trace constituents. *Atmospheric chemistry and physics: from air pollution to climate change*. John Wiley & Sons, Hoboken
- Cummings LE, Stewart JD, Kremer P, Shakya KM (2022) Predicting citywide distribution of air pollution using mobile monitoring and three-dimensional urban structure. *Sustain Cities Soc* 76:103510. <https://doi.org/10.1016/j.scs.2021.103510>
- Liu Y, Xu X, Yang X, He J, Zhang W, Liu X, Ji D, Wang Y (2022) Significant contribution of secondary particulate matter to recurrent air pollution: evidence from in situ observation in the most polluted city of Fen-Wei Plain of China. *J Environ Sci*. <https://doi.org/10.1016/j.jes.2021.09.030>
- Mannucci PM, Franchini M (2017) Health effects of ambient air pollution in developing countries. *Int J Environ Res Public Health* 14(9):1048. <https://doi.org/10.3390/ijerph14091048>
- Li M, Zhang Q, Kurokawa Ji, Woo JH, He K, Lu Z, Ohara T, Song Y, Streets DG, Carmichael GR, Cheng Y (2017) MIX: a mosaic Asian anthropogenic emission inventory under the international collaboration framework of the MICS-Asia and HTAP. *Atmos Chem Phys* 17(2):935–963. <https://doi.org/10.5194/acp-17-935-2017>
- Sulaymon ID, Zhang Y, Hopke PK, Hu J, Rupakheti D, Xie X, Zhang Y, Ajibade FO, Hua J, She Y (2021) Influence of transboundary air pollution and meteorology on air quality in three major cities of Anhui Province China. *J Clean Prod* 329:129641. <https://doi.org/10.1016/j.jclepro.2021.129641>
- Li B, Shi XF, Liu YP, Lu L, Wang GL, Thapa S, Sun XZ, Fu DL, Wang K, Qi H (2020) Long-term characteristics of criteria air pollutants in megacities of Harbin-Changchun megalopolis, Northeast China: Spatiotemporal variations, source analysis, and meteorological effects. *Environ Pollut* 267:115441. <https://doi.org/10.1016/j.envpol.2020.115441>
- Rupakheti D, Yin X, Rupakheti M, Zhang Q, Li P, Rai M, Kang S (2021) Spatio-temporal characteristics of air pollutants over Xinjiang Northwestern China. *Environ Pollut* 268:115907. <https://doi.org/10.1016/j.envpol.2020.115907>
- Zhou X, Strezov V, Jiang Y, Kan T, Evans T (2022) Temporal and spatial variations of air pollution across China from 2015 to 2018. *J Environ Sci* 112:161–169. <https://doi.org/10.1016/j.jes.2021.04.025>
- Qin Y, Li J, Gong K, Wu Z, Chen M, Qin M, Huang L, Hu J (2021) Double high pollution events in the Yangtze River Delta from 2015 to 2019: characteristics, trends, and meteorological situations. *Sci Total Environ*. <https://doi.org/10.1016/j.scitotenv.2021.148349>
- Ding A, Huang X, Nie W, Chi X, Xu Z, Zheng L, Xu Z, Xie Y, Qi X, Shen Y, Sun P (2019) Significant reduction of PM<sub>2.5</sub> in eastern China due to regional-scale emission control: evidence from SORPES in 2011–2018. *Atmos Chem Phys* 19(18):11791–11801. <https://doi.org/10.5194/acp-19-11791-2019>
- Gong S, Liu Y, He J, Zhang L, Lu S, Zhang X (2022) Multi-scale analysis of the impacts of meteorology and emissions on PM<sub>2.5</sub> and O<sub>3</sub> trends at various regions in China from 2013 to 2020: synoptic circulation patterns and pollution. *Sci Total Environ*. <https://doi.org/10.1016/j.scitotenv.2021.152770>
- Lu H, Xie M, Liu X, Liu B, Liu C, Zhao X, Du Q, Wu Z, Gao Y, Xu L (2022) Spatial-temporal characteristics of particulate matters and different formation mechanisms of four typical haze cases in a mountain city. *Atmos Environ* 269:118868. <https://doi.org/10.1016/j.atmosenv.2021.118868>
- Zhang J, Yuan Q, Liu L, Wang Y, Zhang Y, Xu L, Pang Y, Zhu Y, Niu H, Shao L, Yang S (2021) Trans-regional transport of haze particles from the North China Plain to Yangtze River Delta during winter. *J Geophys Res Atmos* 126(8):e2020JD03778. <https://doi.org/10.1029/2020JD03778>
- Duan L, Xiu G, Feng L, Cheng N, Wang C (2016) The mercury species and their association with carbonaceous compositions, bromine and iodine in PM<sub>2.5</sub> in Shanghai. *Chemosphere* 146:263–271. <https://doi.org/10.1016/j.chemosphere.2015.11.058>
- Hong Q, Xie Z, Liu C, Wang F, Xie P, Kang H, Xu J, Wang J, Wu F, He P, Mou F (2016) Speciated atmospheric mercury on haze and non-haze days in an inland city in China. *Atmos Chem Phys* 16(21):13807–13821. <https://doi.org/10.5194/acp-16-13807-2016>
- Javed Z, Tanvir A, Bilal M, Su W, Xia C, Rehman A, Zhang Y, Sandhu O, Xing C, Ji X, Xie M (2021) Recommendations for HCHO and SO<sub>2</sub> retrieval settings from MAX-DOAS observations under different meteorological conditions. *Remote Sens* 13(12):2244. <https://doi.org/10.3390/rs13122244>
- Dai H, Zhu J, Liao H, Li J, Liang M, Yang Y, Yue X (2021) Co-occurrence of ozone and PM<sub>2.5</sub> pollution in the Yangtze River Delta over 2013–2019: Spatiotemporal distribution and meteorological conditions. *Atmos Res* 249:5363. <https://doi.org/10.1016/j.atmosres.2020.105363>
- Wang Y, Gao W, Wang S, Song T, Gong Z, Ji D, Wang L, Liu Z, Tang G, Huo Y, Tian S (2020) Contrasting trends of PM<sub>2.5</sub> and surface-ozone

- concentrations in China from 2013 to 2017. *Nat Sci Rev* 7(8):1331–1339. <https://doi.org/10.1093/nsr/nwaa032>
24. Gao D, Xie M, Chen X, Wang T, Liu J, Xu Q, Mu X, Chen F, Li S, Zhuang B, Li M (2020) Systematic classification of circulation patterns and integrated analysis of their effects on different ozone pollution levels in the Yangtze River Delta Region. *China Atmos Environ* 242:117760. <https://doi.org/10.1016/j.atmosenv.2020.117760>
  25. Hu J, Wang Y, Ying Q, Zhang H (2014) Spatial and temporal variability of PM<sub>2.5</sub> and PM<sub>10</sub> over the North China Plain and the Yangtze River Delta. *China Atmos Environ* 95:598–609. <https://doi.org/10.1016/j.atmosenv.2014.07.019>
  26. Liu X, Zhu B, Kang H, Hou X, Gao J, Kuang X, Yan S, Shi S, Fang C, Pan C, Meng K (2021) Stable and transport indices applied to winter air pollution over the Yangtze River Delta China. *Env Pollut* 272:115954. <https://doi.org/10.1016/j.envpol.2020.115954>
  27. Wang HL, Qiao LP, Lou SR, Zhou M, Ding AJ, Huang HY, Chen JM, Wang Q, Tao SK, Chen CH, Li L (2016) Chemical composition of PM<sub>2.5</sub> and meteorological impact among three years in urban Shanghai China. *J Clean Prod* 112:1302–1311. <https://doi.org/10.1016/j.jclepro.2015.04.099>
  28. National Bureau of Statistics of China (NBSC). <http://www.stats.gov.cn/tjsj/pcsj/rkpc/decrcp/>. Accessed 26 Dec 2021.
  29. Sulaymon ID, Zhang Y, Hopke PK, Hu J, Zhang Y, Li L, Mei X, Gong K, Shi Z, Zhao B, Zhao F (2021) Persistent high PM<sub>2.5</sub> pollution driven by unfavorable meteorological conditions during the COVID-19 lockdown period in the Beijing-Tianjin-Hebei region China. *Environ Res* 198:1186. <https://doi.org/10.1016/j.envres.2021.111186>
  30. He J, Gong S, Yu Y, Wu L, Wu L, Mao H, Song C, Zhao S, Liu H, Li X, Li R (2017) Air pollution characteristics and their relation to meteorological conditions during 2014–2015 in major Chinese cities. *Environ Pollut* 223:484–496. <https://doi.org/10.1016/j.envpol.2017.01.050>
  31. Javed Z, Liu C, Khokhar MF, Xing C, Tan W, Subhani MA, Rehman A, Tanvir A (2019) Investigating the impact of Glyoxal retrieval from MAX-DOAS observations during haze and non-haze conditions in Beijing. *J Environ Sci* 80:296–305. <https://doi.org/10.1016/j.jes.2019.01.008>
  32. Lewis-Beck MS (1994) Factor analysis and related techniques. Sage
  33. Filonchik M, Yan H (2018) The characteristics of air pollutants during different seasons in the urban area of Lanzhou Northwest China. *Environ Earth Sci* 77(22):1–17. <https://doi.org/10.1007/s12665-018-7925-1>
  34. Stein AF, Draxler RR, Rolph GD, Stunder BJ, Cohen MD, Ngan F (2015) NOAA's HYSPLIT atmospheric transport and dispersion modeling system. *Bull Am Meteor Soc* 96(12):2059–2077. <https://doi.org/10.1175/BAMS-D-14-00110.1>
  35. Fleming ZL, Monks PS, Manning AJ (2012) Untangling the influence of air-mass history in interpreting observed atmospheric composition. *Atmos Res* 104:1–39. <https://doi.org/10.1016/j.atmosres.2011.09.009>
  36. Bilal M, Mhawish A, Nichol JE, Qiu Z, Nazeer M, Ali MA, de Leeuw G, Levy RC, Wang Y, Chen Y, Wang L (2021) Air pollution scenario over Pakistan: characterization and ranking of extremely polluted cities using long-term concentrations of aerosols and trace gases. *Remote Sens Environ* 264:112617. <https://doi.org/10.1016/j.rse.2021.112617>
  37. Feng Z, Zheng F, Liu Y, Fan X, Yan C, Zhang Y, Daellenbach KR, Bianchi F, Petäjä T, Kulmala M, Bao X (2022) Evolution of organic carbon during COVID-19 lockdown period: possible contribution of nocturnal chemistry. *Sci Total Environ* 808:152191. <https://doi.org/10.1016/j.scitotenv.2021.152191>
  38. Cheng M, Jiang H, Guo Z (2012) Evaluation of long-term tropospheric NO<sub>2</sub> columns and the effect of different ecosystem in Yangtze River Delta. *Procedia Environ Sci* 13:1045–1056. <https://doi.org/10.1016/j.proenv.2012.01.098>
  39. Liu F, Zhang Q, Zheng B, Tong D, Yan L, Zheng Y, He K (2016) Recent reduction in NO<sub>x</sub> emissions over China: synthesis of satellite observations and emission inventories. *Environ Res Lett* 11(11):114002. <https://doi.org/10.1088/1748-9326/11/11/114002>
  40. Wang Y, Ali M, Bilal M, Qiu Z, Mhawish A, Almazroui M, Shahid S, Islam MN, Zhang Y, Haque M (2021) Identification of NO<sub>2</sub> and SO<sub>2</sub> pollution hot-spots and sources in Jiangsu Province of China. *Remote Sens* 13(18):3742. <https://doi.org/10.3390/rs13183742>
  41. Zhang L, Lee CS, Zhang R, Chen L (2017) Spatial and temporal evaluation of long-term trend (2005–2014) of OMI retrieved NO<sub>2</sub> and SO<sub>2</sub> concentrations in Henan Province, China. *Atmos Environ* 154:151–166. <https://doi.org/10.1016/j.atmosenv.2016.11.067>
  42. Zhang NN, Ma F, Qin CB, Li YF (2018) Spatiotemporal trends in PM<sub>2.5</sub> levels from 2013 to 2017 and regional demarcations for joint prevention and control of atmospheric pollution in China. *Chemosphere* 210:1176–1184. <https://doi.org/10.1016/j.chemosphere.2018.07.142>
  43. Li K, Jacob DJ, Liao H, Shen L, Zhang Q, Bates KH (2019) Anthropogenic drivers of 2013–2017 trends in summer surface ozone in China. *Proc Natl Acad Sci* 116(2):422–427. <https://doi.org/10.1073/pnas.1812168116>
  44. Yin H, Lu X, Sun Y, Li K, Gao M, Zheng B, Liu C (2021) Unprecedented decline in summertime surface ozone over eastern China in 2020 comparably attributable to anthropogenic emission reductions and meteorology. *Environ Res Lett* 16(12):124069. <https://doi.org/10.1088/1748-9326/ac3e22>
  45. Wang W, der Vander AR, Ding J, van Weele M, Cheng T (2021) Spatial and temporal changes of the ozone sensitivity in China based on satellite and ground-based observations. *Atmos Chem Phys* 21(9):7253–7269. <https://doi.org/10.5194/acp-21-7253-2021>
  46. The Chinese ministry of environmental and ecology, the volatile organic compound management attack program in 2020. [www.mee.gov.cn/xxgk2018/xxgk/xxgk03/202006/t20200624\\_785827.html](http://www.mee.gov.cn/xxgk2018/xxgk/xxgk03/202006/t20200624_785827.html)
  47. Javed Z, Wang Y, Xie M, Tanvir A, Rehman A, Ji X, Xing C, Shakoor A, Liu C (2020) Investigating the impacts of the COVID-19 lockdown on trace gases using ground-based MAX-DOAS observations in Nanjing China. *Remote Sens* 12(23):3939
  48. Javed Z, Tanvir A, Wang Y, Waqas A, Xie M, Abbas A, Sandhu O, Liu C (2021) Quantifying the impacts of COVID-19 lockdown and spring festival on air quality over Yangtze river delta region. *Atmosphere* 12(6):735. <https://doi.org/10.3390/atmos12060735>
  49. Li L, Li Q, Huang L, Wang Q, Zhu A, Xu J, Liu Z, Li H, Shi L, Li R, Azari M (2020) Air quality changes during the COVID-19 lockdown over the Yangtze river delta region: an insight into the impact of human activity pattern changes on air pollution variation. *Sci Total Environ* 732:139282. <https://doi.org/10.1016/j.scitotenv.2020.139282>
  50. Sun Y, Zhuang G, Tang A, Wang Y, An Z (2006) Chemical characteristics of PM<sub>2.5</sub> and PM<sub>10</sub> in haze-fog episodes in Beijing. *Environ Sci Technol* 40(10):3148–3155. <https://doi.org/10.1021/es051533g>
  51. Xiao ZM, Zhang YF, Hong SM, Bi XH, Jiao L, Feng YC, Wang YQ (2011) Estimation of the main factors influencing haze, based on a long-term monitoring campaign in Hangzhou China. *Aerosol Air Qual Res* 11(7):873–882. <https://doi.org/10.4209/aaqr.2011.04.0052>
  52. Lv M, Li Z, Jiang Q, Chen T, Wang Y, Hu A, Cribb M, Cai A (2021) Contrasting trends of surface PM<sub>2.5</sub>, O<sub>3</sub>, and NO<sub>2</sub> and their relationships with meteorological parameters in typical coastal and inland cities in the Yangtze River Delta. *Int J Environ Res Pub Health* 18(23):12471. <https://doi.org/10.3390/ijerph182312471>
  53. Tanvir A, Javed Z, Jian Z, Zhang S, Bilal M, Xue R, Wang S, Bin Z (2021) Ground-based MAX-DOAS observations of tropospheric NO<sub>2</sub> and HCHO during COVID-19 lockdown and spring festival over Shanghai China. *Remote Sens* 13(3):488. <https://doi.org/10.3390/rs13030488>
  54. Yue X, Unger N, Harper K, Xia X, Liao H, Zhu T, Xiao J, Feng Z, Li J (2017) Ozone and haze pollution weakens net primary productivity in China. *Atmos Chem Phys* 17(9):6073–6089. <https://doi.org/10.5194/acp-17-6073-2017>
  55. Ma S, Xiao Z, Zhang Y, Wang L, Shao M (2020) Assessment of meteorological impact and emergency plan for a heavy haze pollution episode in a core city of the North China Plain. *Aerosol Air Qual Res* 20(1):26–42. <https://doi.org/10.4209/aaqr.2019.08.0392>
  56. Zhang H, Wang Y, Hu J, Ying Q, Hu XM (2015) Relationships between meteorological parameters and criteria air pollutants in three megacities in China. *Environ Res* 140:242–254. <https://doi.org/10.1016/j.envres.2015.04.004>
  57. Chen H, Zhuang B, Liu J, Wang T, Li S, Xie M, Li M, Chen P, Zhao M (2019) Characteristics of ozone and particles in the near-surface atmosphere in the urban area of the Yangtze River Delta China. *Atmos Chem Phys* 19(7):4153–4175. <https://doi.org/10.5194/acp-19-4153-2019>
  58. Hama SM, Kumar P, Harrison RM, Bloss WJ, Khare M, Mishra S, Namdeo A, Sokhi R, Goodman P, Sharma C (2020) Four-year assessment of ambient particulate matter and trace gases in the Delhi-NCR region of India. *Sustain Cities Soc* 54:102003. <https://doi.org/10.1016/j.scs.2019.102003>
  59. Zhao C, Wang Y, Shi X, Zhang D, Wang C, Jiang JH, Zhang Q, Fan H (2019) Estimating the contribution of local primary emissions to particulate

- pollution using high-density station observations. *J Geophys Res Atmos* 124(3):1648–1661. <https://doi.org/10.1029/2018JD028888>
60. Zhang YL, Cao F (2015) Fine particulate matter (PM 25) in China at a city level. *Sci Rep* 5(1):1–12. <https://doi.org/10.1038/srep14884>
61. Yang G, Liu Y, Li X (2020) Spatiotemporal distribution of ground-level ozone in China at a city level. *Sci Rep* 10(1):1–12. <https://doi.org/10.1038/s41598-020-64111-3>
62. Zhao H, Chen K, Liu Z, Zhang Y, Shao T, Zhang H (2021) Coordinated control of PM<sub>2.5</sub> and O<sub>3</sub> is urgently needed in China after implementation of the “Air pollution prevention and control action plan.” *Chemosphere* 270:9441. <https://doi.org/10.1016/j.chemosphere.2020.129441>
63. Chen Z, Zhuang Y, Xie X, Chen D, Cheng N, Yang L, Li R (2019) Understanding long-term variations of meteorological influences on ground ozone concentrations in Beijing During 2006–2016. *Environ Pollut* 245:29–37. <https://doi.org/10.1016/j.envpol.2018.10.117>
64. Zhang G, Xu H, Qi B, Du R, Gui K, Wang H, Jiang W, Liang L, Xu W (2018) Characterization of atmospheric trace gases and particulate matter in Hangzhou China. *Atmos Chem Phys* 18(3):1705–1728. <https://doi.org/10.5194/acp-17-6073-2017>
65. Niu Z, Hu T, Kong L, Zhang W, Rao P, Ge D, Zhou M, Duan Y (2021) Air-pollutant mass concentration changes during COVID-19 pandemic in Shanghai, China. *Air Qual Atmos Health* 14(4):523–532
66. Li K, Ni R, Jiang T, Tian Y, Zhang X, Li C, Xie C (2022) The regional impact of the COVID-19 lockdown on the air quality in Ji’nan China. *Scient Rep* 12(1):1–12
67. Zhang L, An J, Liu M, Li Z, Liu Y, Tao L, Liu X, Zhang F, Zheng D, Gao Q, Guo X (2020) Spatiotemporal variations and influencing factors of PM<sub>2.5</sub> concentrations in Beijing China. *Environ Pollut* 262:4276. <https://doi.org/10.1016/j.envpol.2020.114276>
68. Mandal J, Chanda A, Samanta S (2022) Air pollution in three megacities of India during the Diwali festival amidst COVID-19 pandemic. *Sustain Cities Soc* 76:103504. <https://doi.org/10.1016/j.scs.2021.103504>
69. Zhou B, Yu L, Zhong S, Bian X (2018) The spatiotemporal inhomogeneity of pollutant concentrations and its dependence on regional weather conditions in a coastal city of China. *Environ Monit Assess* 190(5):1–17. <https://doi.org/10.1007/s10661-018-6623-5>
70. Mhawish A, Banerjee T, Sorek-Hamer M, Bilal M, Lyapustin AI, Chatfield R, Broday DM (2020) Estimation of high-resolution PM<sub>2.5</sub> over the Indo-Gangetic plain by fusion of satellite data, meteorology, and land use variables. *Environ Sci Technol* 54(13):7891–7900. <https://doi.org/10.1021/acs.est.0c01769>

## Publisher’s Note

Springer Nature remains neutral with regard to jurisdictional claims in published maps and institutional affiliations.

Submit your manuscript to a SpringerOpen<sup>®</sup> journal and benefit from:

- Convenient online submission
- Rigorous peer review
- Open access: articles freely available online
- High visibility within the field
- Retaining the copyright to your article

---

Submit your next manuscript at ► [springeropen.com](https://www.springeropen.com)

---